

Electronic Supplementary Information

Biomimetic molecular organization of naphthalene diimide in the solid state: tunable (chiro-) optical, viscoelastic and nanoscale properties

M. Pandeeswar,^a Harshavardhan Khare,^b Suryanarayananarao Ramakumar,^b and T. Govindaraju^{*a}

^a*Bioorganic Chemistry Laboratory, New Chemistry Unit, Jawaharlal Nehru Centre for Advanced Scientific Research, Jakkur P.O., Bangalore 560064, India. Fax: +91 80 22082627; E-mail: tgraju@jncasr.ac.in*

^b*Department of Physics, Indian Institute of Science, Bangalore-560012, India.*

Contents

Experimental section

Materials and methods

Synthetic procedure and characterization

Crystallographic information of eNe

Crystallographic information of L-ANA

Crystallographic information of D-ANA

Crystallographic information of L-FNF

Crystallographic information of D-FNF

Crystallographic information of L-WNW

UV-vis absorption spectra recorded in thin film

UV-vis absorption spectra recorded in solution

Excitation spectra of NDI conjugates

FESEM micrographs of solutions

¹HNMR and ¹³C NMR spectra

HRMS spectra

References

1. Materials and methods

Materials: 1,4,5,8-Naphthalenetetracarboxylic dianhydride (NDA), triethylamine and amino acids were obtained from Sigma-Aldrich. All other reagents and solvents were of reagent grade and used without further purification.

Absorption Spectroscopy: UV-vis spectra were recorded on a Perkin Elmer Model Lambda 900 spectrophotometer by using quartz cuvette of 1 mm path length. Solvent systems I=MCH:THF = 80:20 (V/V), II=DMSO, III= MCH:CHCl₃ = 80:20 (V/V)). Diffused reflectance measurements were performed on the solid powder sample with BaSO₄ as a reference and converted in to pseudo-absorbance spectra using Kubelka-Munk function as follows

$$f^{km} = \frac{(1-R(hv))^2}{2R(hv)} = \frac{\alpha(hv)}{S}$$

where $R(hv)$ is the reflectance of the sample measured vs. 100% reflectivity standard, $\alpha(hv)$ is the absorption coefficient and S stands for the scattering factor of the mixture, which practically is equal to scattering factor.

Fluorescence Spectroscopy: Fluorescence spectra were recorded on a Perkin Elmer Model LS 55 spectrophotometer. All fluorescence spectra with excitation wavelength $\lambda_{ex} = 380$ nm.

Circular Dichroism (CD): CD measurements were carried out on a Jasco J-815 spectropolarimeter under nitrogen atmosphere by using quartz cuvette of 1 mm path length. Solvent systems I=MCH:THF = 80:20 (V/V)), II=DMSO, III= MCH:CHCl₃ = 80:20 (V/V))

NMR Spectroscopy: ¹H and ¹³C NMR spectra were recorded on a Bruker AV-400 spectrometer with chemical shifts reported as ppm (in CDCl₃/DMSO-*d*₆ with tetramethylsilane as internal standard).

Mass Spectrometry (MS): High resolution mass spectra (HRMS) were obtained from on Agilent Technologies 6538 UHD Accurate-Mass Q-TOF LC/MS spectrometer.

Field Emission Scanning Electron Microscopy (FESEM): FESEM images were acquired with a FEI Nova nanoSEM-600 equipped with a field-emission gun operating at 15 kV. The

xerogels were prepared by transfer of organogels onto a Si (111) substrate and dried in air followed by vacuum drying at room temperature.

Fluorescence confocal microscopy: Fluorescence confocal microscopy images were obtained from LSM 510 META-Carl Zeiss. A 365 nm laser was employed to excite the crystals.

Gelation Experiments: Methylcyclohexene (MCH) was added to the solution of amino acid – naphthalene diimide (NDI) conjugate in tetrahydrofuran (THF)/chloroform to make 6 mM under ultrasonication (MCH:(THF/CHCl₃) = 80:20 (v/v)). After few minutes the formation of organogels was observed. The gel formation is determined by tilting or inverting the sample vial upside down.

Rheology studies: Amplitude and frequency sweeps were performed on a Anton Paar rheometer MCR302 SN000000; ID80963516; FW3.65; Slot(11,-1) series device. All the measurements were performed at room temperature.

Time-correlated Single Photon Counting (TCSPC) studies: Fluorescence decay profiles were performed using FLSP 920 spectrometer, Edinburgh Instrument. EPLED.

Crystallographic data and structure refinement details

Crystal growth: Crystals were grown at room temperature in DMSO as solvent.

Data collection: Data collection was done on Bruker AXS SMART APEX Single Crystal Diffractometer: All the datasets were collected at 100 K.

Structure solution and refinement: SHELXS-2013¹ and SHELXL-2013² programs were used to solve and refine the X-ray diffraction data. WinGx package (version 1.80.05)³ was used as front end to SHELX programs.

Experimental section

General procedure for the synthesis of amino acid and ethylamine conjugated NDIs (ANA, FNF, WNW and eNe).

1,4,5,8- Naphthalenetetracarboxylic dianhydride (NDA) (0.5 g, 1.8 mmol) and corresponding amino acid (0.6 g, 3.7 mmol) were suspended in 10 mL of dimethylformamide (DMF). To this suspension, triethylamine (TEA) (0.2 mL) was added and allowed to reflux for 12 h. After cooling to room temperature the reaction mixture was added into 500 mL of 2N HCl and was stirred for 1 h. The precipitate was collected through suction funnel, washed with excess of distilled water (to remove excess HCl) and dried under vacuo to obtain amino acid-naphthalene diimide (NDI) conjugates (L-ANA, D-ANA, L-FNF, D-FNF, L-WNW, and D-WNW) in quantitative yield. To prepare eNe, 1,4,5,8- naphthalenetetracarboxylicdianhydride (0.5 g, 1.8 mmol) and ethylamine (0.2 mL, 3.7 mmol) were suspended in 10 mL of dimethylformamide (DMF). To this suspension, triethylamine (TEA) (0.2 mL) was added and allowed to reflux for 12 h. After cooling to room temperature the precipitate was collected through suction funnel, washed with excess of distilled water (to remove TEA), and dried under vacuo to obtain the product in quantitative yield.

Characterization data for amino acid-NDI conjugates

L-ANA: Yield 73.2%; mp 345-348 °C; ¹H NMR (*DMSO-d*₆, 400 MHz) δ_H 12.85 (2H, s), 8.71 (4H, s), 5.6 (2H, dd), 1.57 (6H, d); ¹³C NMR (*DMSO-d*₆, 100 MHz) δ_C 171.0, 162.0, 130.9, 126.1, 49.0, 14.3; HRMS: m/z calcd for [M+H]⁺ [C₂₀H₁₄N₂O₈+H], 411.0828; found 411.0853.

D-ANA: Yield 73.2%; mp 345-348 °C; ¹H NMR (*DMSO-d*₆, 400 MHz) δ_H 12.84 (2H, s), 8.71 (4H, s), 5.6 (2H, dd), 1.57 (6H, d); ¹³C NMR (*DMSO-d*₆, 100 MHz) δ_C 171.0, 162.0, 130.9, 126.1, 49.0, 14.3; HRMS: calcd for [M+H]⁺ [C₂₀H₁₄N₂O₈+H], 411.0828; found 411.0816.

L-FNF: Yield: 70%; mp 170-173 °C; ¹H NMR (*DMSO-d*₆, 400 MHz) δ_H 12.88 (2H, s), 8.64 (4H, s), 7.18-7.02 (10H, m), 5.85 (2H, dd), 3.61 (2H, dd), 3.50 (2H, dd); ¹³C NMR (*DMSO-d*₆, 100 MHz) δ_C 170.1, 161.9, 137.8, 131.2, 128.9, 128.1, 126.3, 126.0, 125.6, 54.5, 34.2; HRMS: calcd for [M+H]⁺ [C₃₂H₂₂N₂O₈+H], 563.1454; found 563.1477.

D-FNF: Yield: 70%; mp 170-173 °C; ¹H NMR (*DMSO-d*₆, 400 MHz) δ_H 13.04 (2H, s), 8.64 (4H, s), 7.17-7.03 (10H, m), 5.85 (2H, dd), 3.60 (2H, dd), 3.35 (2H, dd); ¹³C NMR (*DMSO-d*₆, 100 MHz) δ_C 170.1, 161.9, 137.7, 131.2, 128.9, 128.1, 126.3, 126.0, 125.6, 54.5, 34.2; HRMS: calcd for [M+H]⁺ [C₃₂H₂₂N₂O₈+H], 563.1454; found 563.1421.

L-WNW: Yield: 88.6%; mp 220-223 °C; ¹H NMR (*DMSO-d*₆, 400 MHz) δ_H 12.99 (2H, s), 10.64 (2H, d), 8.60 (4H, s), 7.48-6.78 (10H, m), 5.85 (2H, dd), 3.70 (2H, dd), 3.52 (2H, dd); ¹³C NMR (*DMSO-d*₆, 100 MHz) δ_C 170.4, 162.0, 135.8, 131.1, 127.0, 125.9, 125.6, 123.6, 120.7, 118.1, 117.8, 111.2, 110.0, 54.2, 24.0; HRMS: calcd for [M+H]⁺ [C₃₆H₂₄N₄O₈+H], 641.1672; found 641.1653.

D-WNW: Yield: 88.6%; mp 220-223 °C; ¹H NMR (*DMSO-d*₆, 400 MHz) δ_H 13.0 (2H, s), 10.64 (2H, d), 8.60 (4H, s), 7.47-6.78 (10H, m), 5.85 (2H, dd), 3.69 (2H, dd), 3.50 (2H, dd); ¹³C NMR (*DMSO-d*₆, 100 MHz) δ_C 170.4, 162.0, 135.8, 131.1, 127.0, 125.9, 125.6, 123.6, 120.7, 118.1, 117.8, 111.2, 110.0, 54.2, 24.0; HRMS: calcd for [M+H]⁺ [C₃₆H₂₄N₄O₈+H], 641.1672; found 641.1623.

eNe: Yield: 85%; mp 320-322 °C; ¹H NMR (*CDCl*₃+Trifluoroacetic acid(TFA, 3μL), 400 MHz) δ_H 8.81 (4H, s), 4.29 (4H, q), 1.37 (6H, t); ¹³C NMR (*CDCl*₃+TFA(3μL), 100 MHz) δ_C 163.2, 131.4, 126.6, 126.5, 36.5, 13.1; HRMS: calcd for [M+H]⁺ [C₁₈H₁₄N₂O₄+H], 323.1032; found 323.1027.

Crystallographic information of eNe

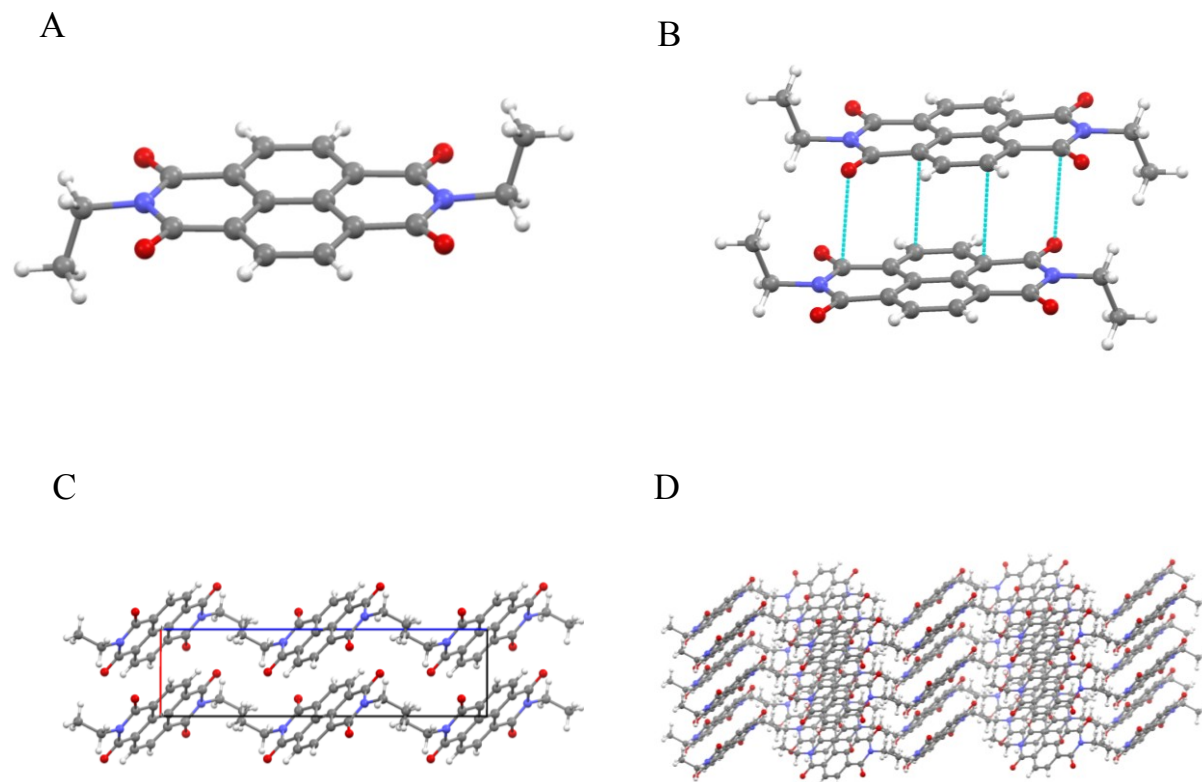


Fig. S1 A) Single molecular geometry of eNe. B) van der Waals contacts between the two successive molecules (cyan doted lines). C) Unit cell viewing along *b* axis. D) Two dimensional slipped stacked packing of molecules.

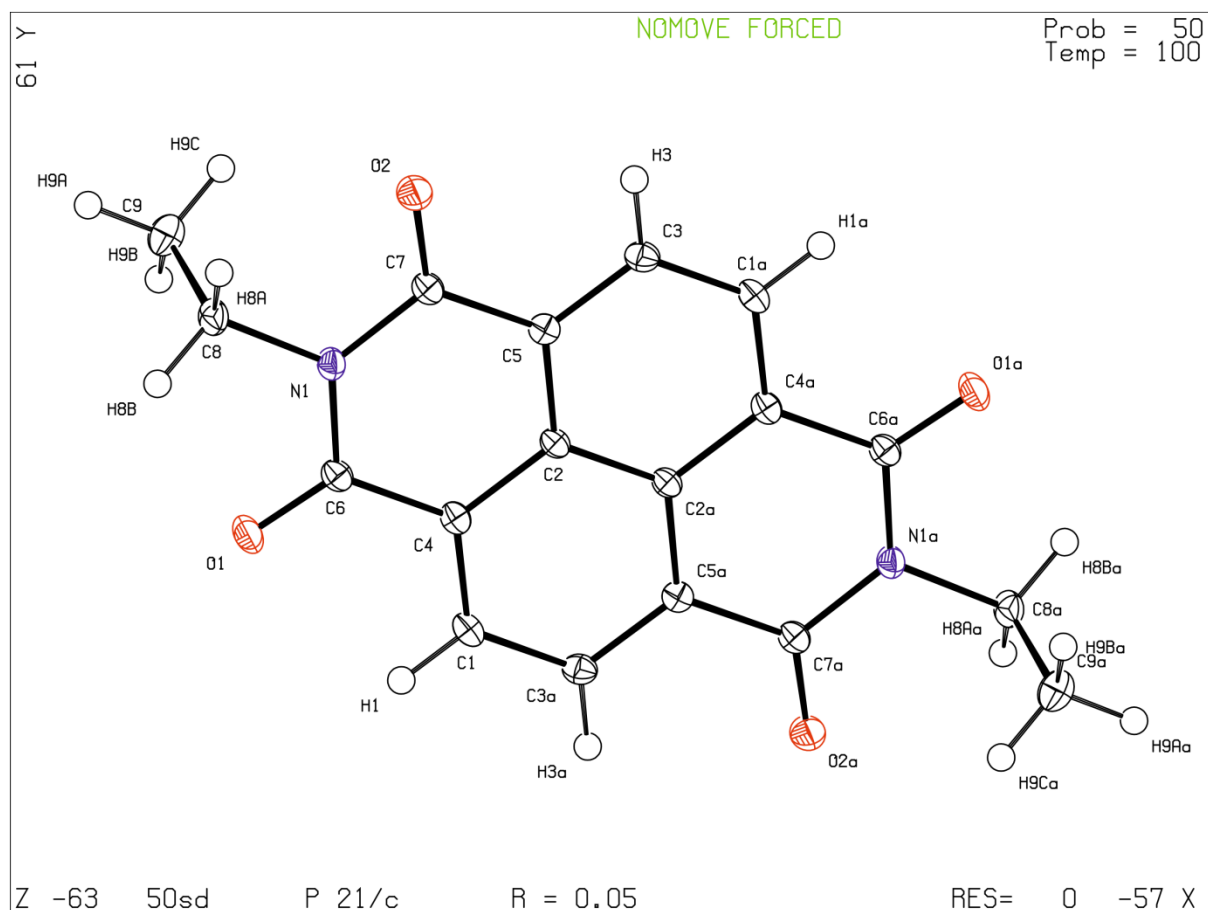


Fig. S2 ORTEP diagram of eNe

List of selected noncovalent interactions in eNe crystal structure

Face to face $\pi\cdots\pi$ stacking: Cofacial stacking of NDI

Ring 1	Ring 2	Distance (Å)	Angle between two NDI planes (°)	Description
NDI core unit	NDI core unit	3.26	0	Side-side overlap

Hydrogen bonds

Donor (D)	Acceptor (A)	D···A Distance (Å)	H···A Distance (Å)	D-H···A Angle (°)	Description
C9H9A	O2	3.26	2.49	135.72	Intermolecular C-H (ethyl sidechain)···O (carbonyl NDI) interactions
C1H1	O1	3.24	2.39	148.50	Intermolecular C-H (Aromatic NDI)···O (carbonyl NDI) interactions

Molecular packing: Slipped stack

Supramolecular tilt angle: 44.63°

Crystallographic information of L-ANA

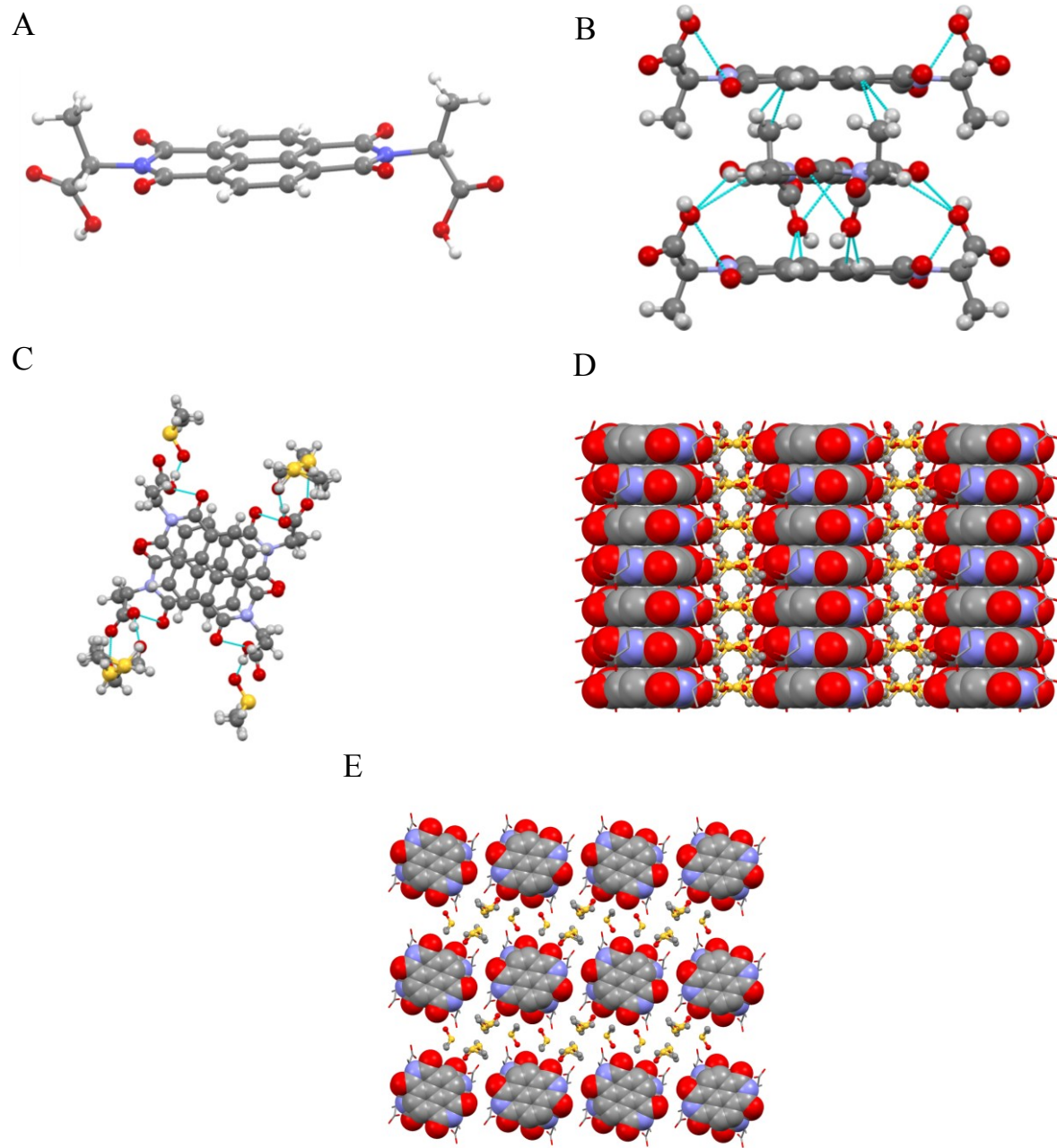


Fig. S3 A) Single molecular geometry of L-ANA indicating the *cis* conformation of c_{α} substituents (methyl) with respect to NDI plane. B) van der Waals contacts between the three successive cofacial columnar π -stacks (cyan doted lines). C) Solvent molecule interaction (cyan doted lines) viewing along crystallographic b axis. D) and E) L-ANA cofacial columnar π -stacks separated by solvent (DMSO) layers; viewed along *a* axis and *b* axis respectively (NDI core spacefill representation).

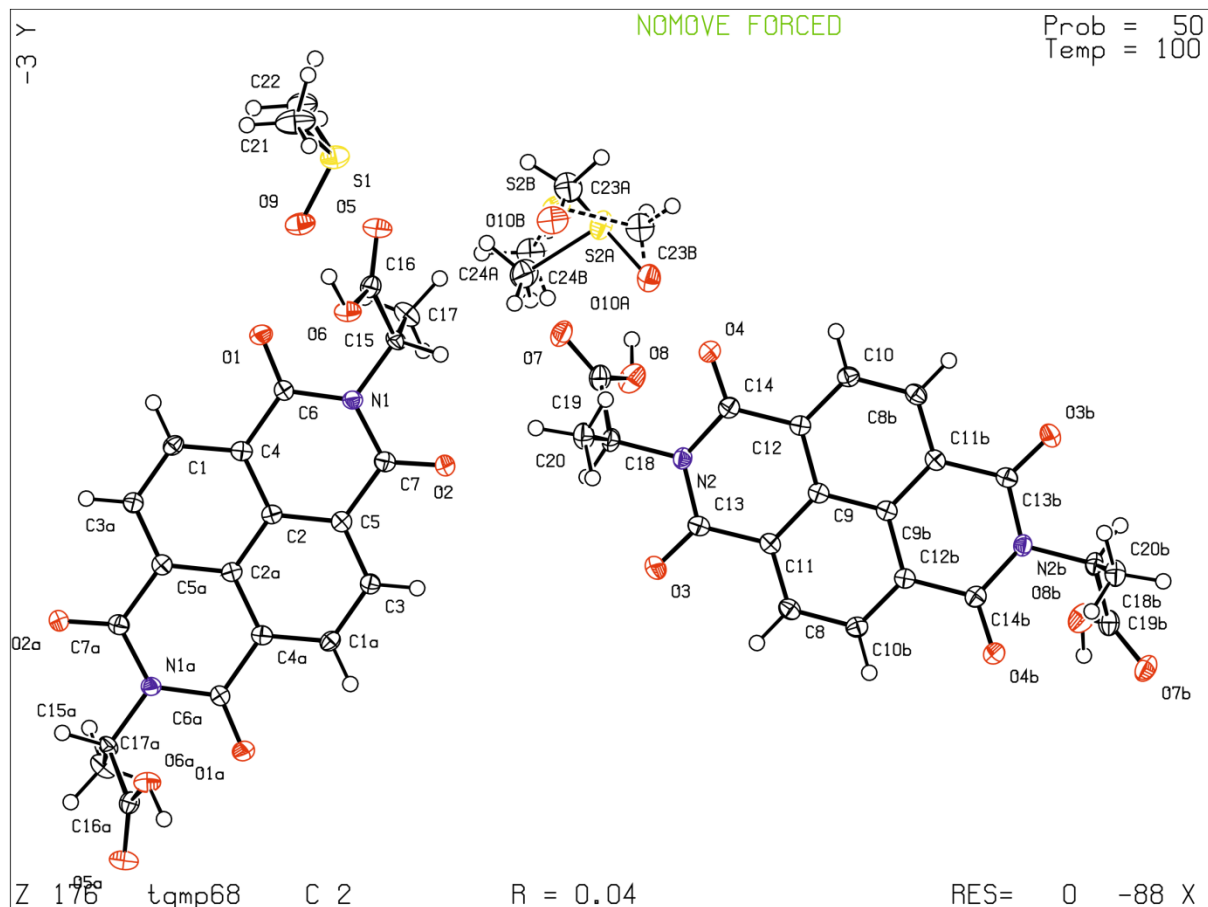


Fig. S4 ORTEP diagram of L-ANA

List of selected noncovalent interactions in L-**ANA** crystal structure

Face to face $\pi\cdots\pi$ stacking: Cofacial stacking of NDI

	Ring 1	Ring 2	Distance (Å)	Angle between two NDI planes (°)
Set 1	NDI core unit	NDI core unit	3.47	0.00
Set 2	NDI core unit	NDI core unit	3.56	0.00

Set-1

van der Waals' contacts

van der Waals' contact	Distance (Å)	Description
C17…H8	2.88	Intermolecular C-H (Alanine sidechain)…H (Aromatic NDI), 2 per set
H17A…H8	2.27	

Set-2

Hydrogen bonds

Donor (D)	Acceptor (A)	D…A Distance (Å)	H…A Distance (Å)	D-H…A Angle (°)	Description
C8H8	O6	3.08	2.39	128.63	Intermolecular C-H (Aromatic NDI)…O (carboxylic acid), 2 per set
C3H3	O8	3.07	2.44	124.35	Intermolecular C-H (Aromatic NDI)…O (carboxylic acid), 2 per set

Cofacial NDI-NDI twist angle = 69.17° (anti-clockwise)

Crystallographic information of D-ANA

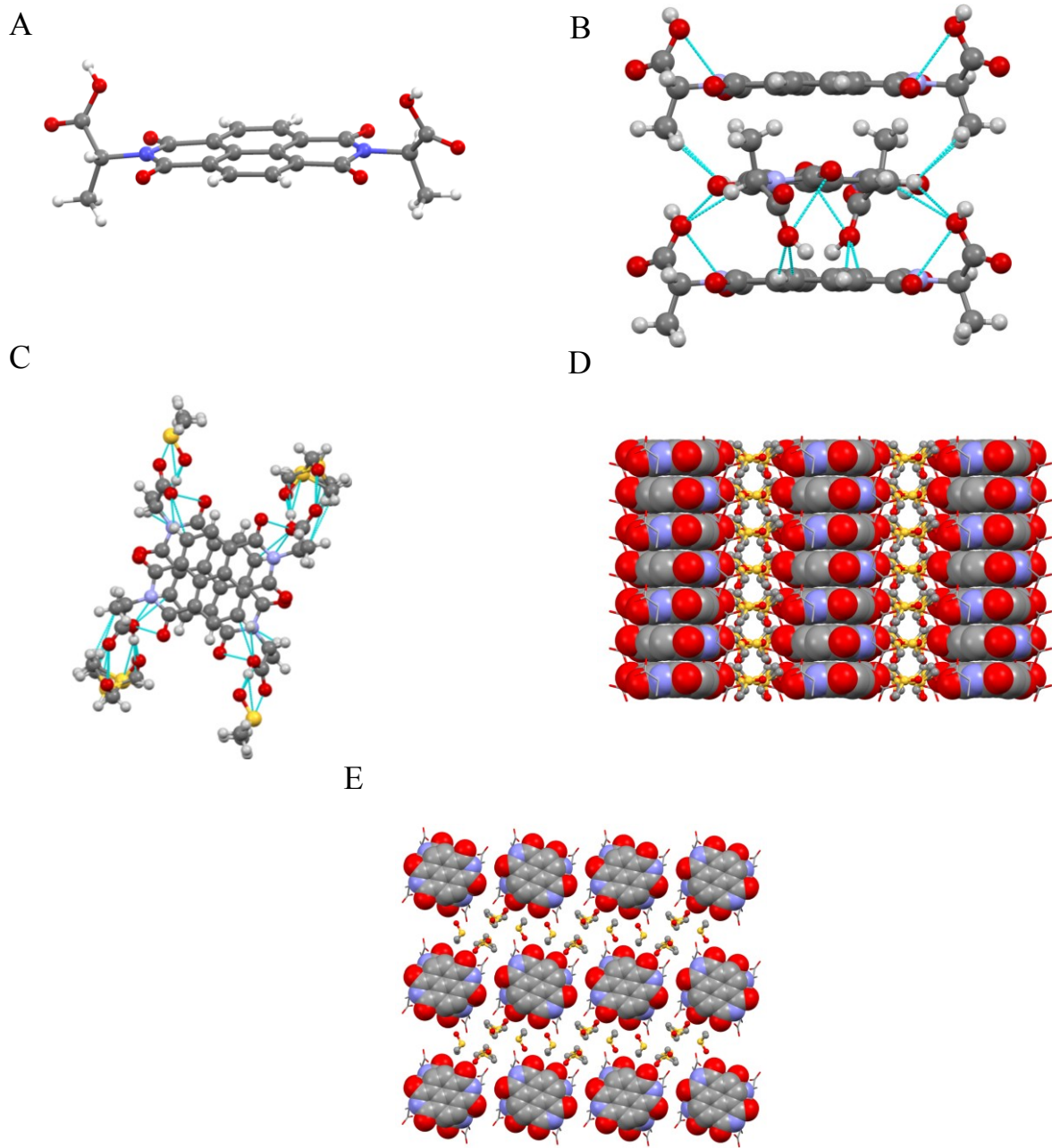


Fig. S5 A) Single molecular geometry of D-ANA indicating the *cis* conformation of c_{α} substituents (methyl) with respect to NDI plan. B) van der Waals contacts between the three successive cofacial columnar π -stacks (cyan doted lines). C) Solvent molecule interaction (cyan doted lines) viewing along crystallographic b axis. D) and E) D-ANA cofacial columnar π -stacks separated by solvent (DMSO) layers; viewed along a axis and b axis respectively (NDI core spacefill representation). In D-E hydrogen atoms have been omitted for the clarity.

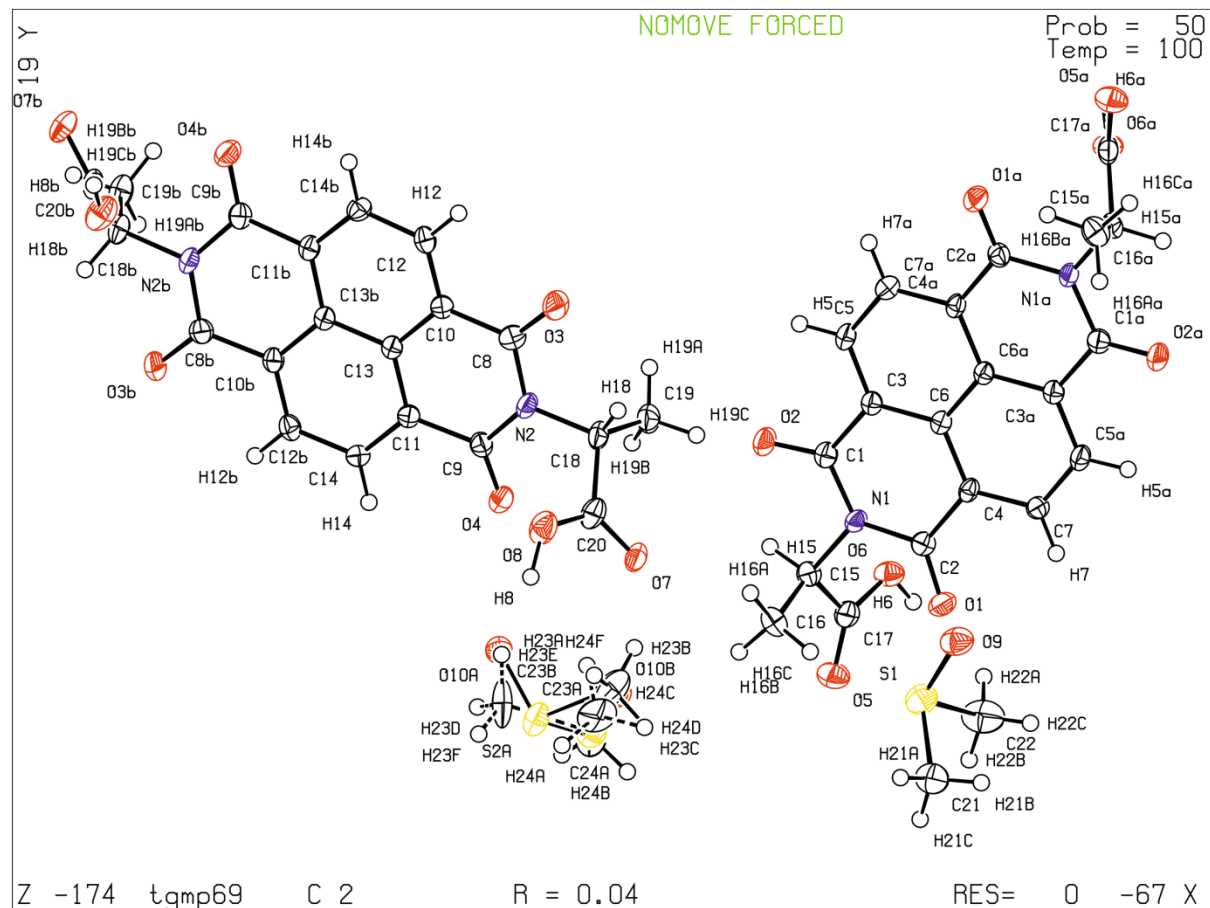


Fig. S6 ORTEP diagram of D-ANA

List of selected noncovalent interactions in D-**ANA** crystal structure

Face to face $\pi\cdots\pi$ stacking: Cofacial stacking of NDI

	Ring 1	Ring 2	Distance (Å)	Angle between two NDI planes (°)
Set 1	NDI core unit	NDI core unit	3.48	0.00
Set 2	NDI core unit	NDI core unit	3.57	0.00

Set-1

van der Waals' contacts

van der Waals' contact	Distance (Å)	Description
C16---H12	2.90	Intermolecular C-H (Alanine sidechain)…H (Aromatic NDI), 2 per set
H16A---H12	2.28	

Set-2

Hydrogen bonds

Donor (D)	Acceptor (A)	D…A Distance (Å)	H…A Distance (Å)	D-H…A Angle (°)	Description
C12H12	O6	3.10	2.42	128.24	Intermolecular C-H(Aromatic NDI)…O (carboxylic acid), 2 per set
C5H5	O8	3.08	2.45	124.34	Intermolecular C-H (Aromatic NDI)…O (carboxylic acid), 2 per set

Cofacial NDI-NDI twist angle = 69.27° (clockwise)

Crystallographic information of L-FNF

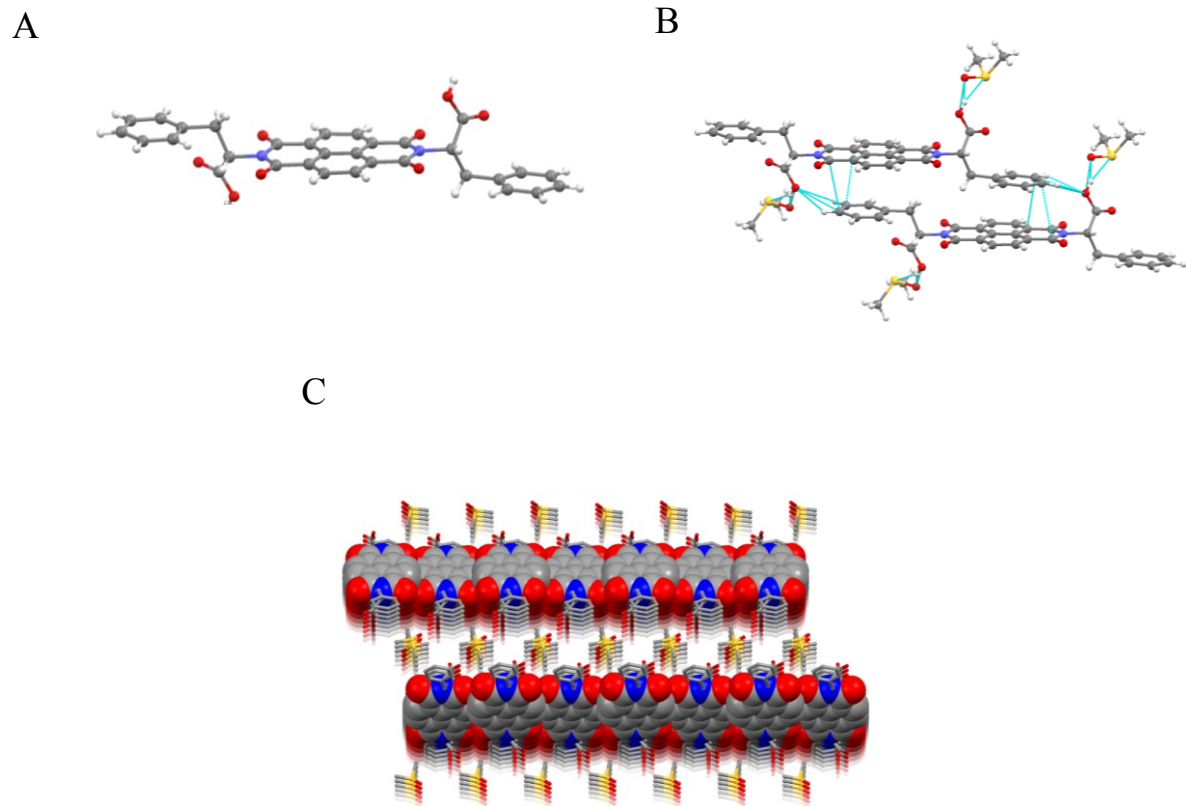


Fig. S7 A) Single molecular geometry of L-FNF indicating the *trans* conformation of c_{α} substituents (phenyl) with respect to NDI plane. B) van der Waals' contacts between the two successive brickwork π -stacks (cyan dotted lines). C) L-FNF layers (NDI core spacefill representation) separated by solvent (DMSO) layers; viewed along a axis. hydrogen atoms have been omitted for the clarity.

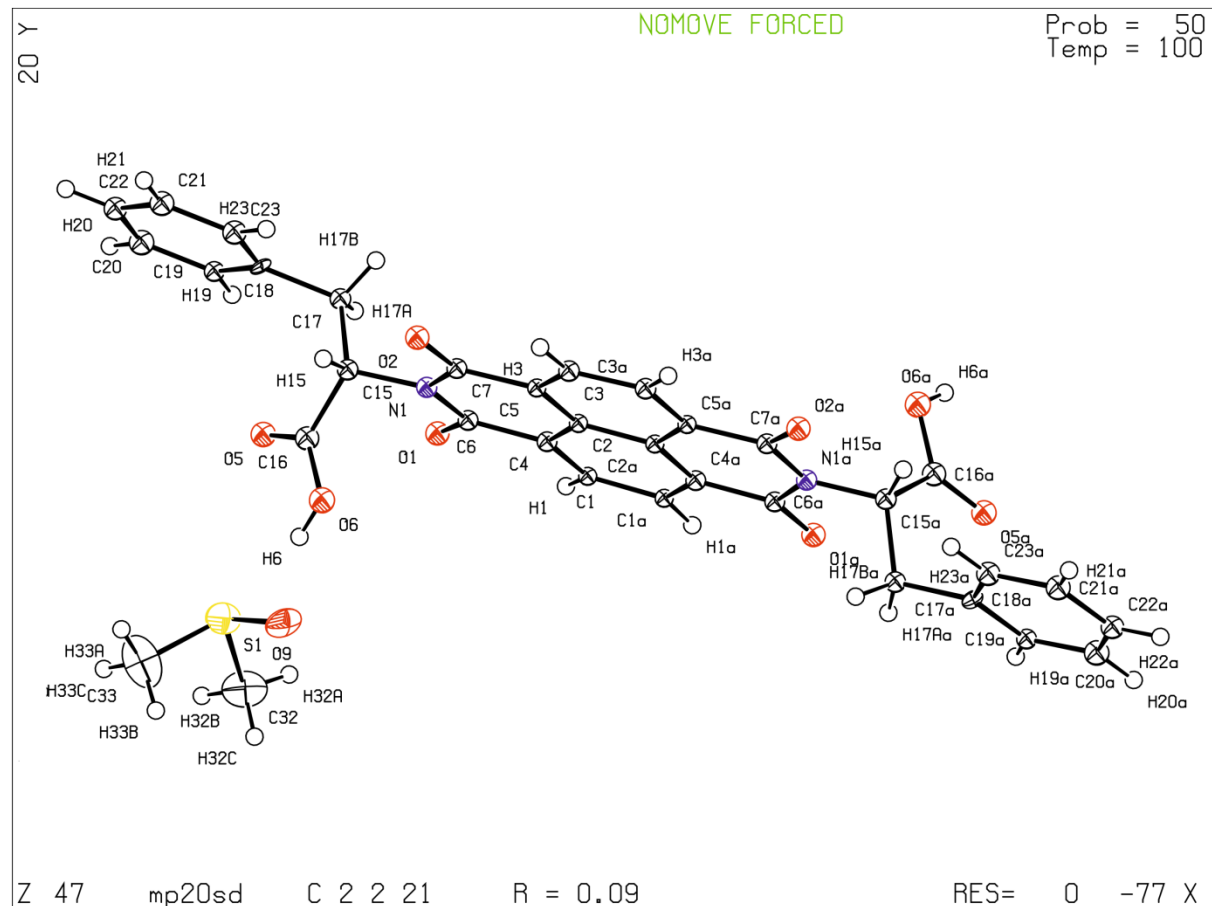


Fig. S8 ORTEP diagram of L-FNF

List of selected noncovalent interactions in L-FNF crystal structure

$\pi \cdots \pi$ stacking

Ring 1	Ring 2	Distance (Å)	Angle between two NDI planes (°)	Description
Phenyl ring (Centroid)	NDI core unit	3.38	3.7	Intermolecular $\pi \cdots \pi$ interactions

Face to Face

Hydrogen bonds

Donor (D)	Acceptor (A)	D···A Distance (Å)	H···A Distance (Å)	D-H···A Angle (°)	Description
C22H22	O6	3.21	2.65	118.35	Aromatic (Phenyl) C -H···O (carboxylic acid) interactions
C20H20	O6	3.18	2.58	121.34	
C3H3	O1	3.28	3.00	98.26	Intermolecular Aromatic (NDI) C-H···O (carbonyl of NDI) interactions
C1H1	O2	3.26	2.90	104.21	
C21H21	O5	3.54	2.60	170.40	Intermolecular Aromatic (Phenyl) C -H···O (carboxylic acid) interactions

Interactions with solvent (DMSO) molecule

Hydrogen bonds

Donor (D)	Acceptor (A)	D···A Distance (Å)	H···A Distance (Å)	D-H···A Angle (°)	Description
O6H6	O9	2.56	1.75	160.81	Intermolecular solvent (DMSO) O···molecule (carboxylic acid) interactions

van der Waals' contacts

van der Waals' contact	Distance (Å)	Description
H33A···H15	2.388	Intermolecular solvent (DMSO) C-H···H-C (α -CH of phenylalanine) interaction

CH···π interactions

CH Donor (D)	π Acceptor (A)	D···A-centroid Distance (Å)	H···A-centroid Distance (Å)	D-H···A-centroid Angle (°)	Description
C32H32A	Phenyl ring	3.900	3.014	150.96	Intermolecular solvent (DMSO) C-H···Phenyl ring (phenylalanine) interaction

Molecular packing

- Intralayer along *b* axis: Brickwork
- Interlayer along *c* axis: Slipped herringbone

Angle between the layers: 66° (anti-clockwise)

Crystallographic information of D-FNF

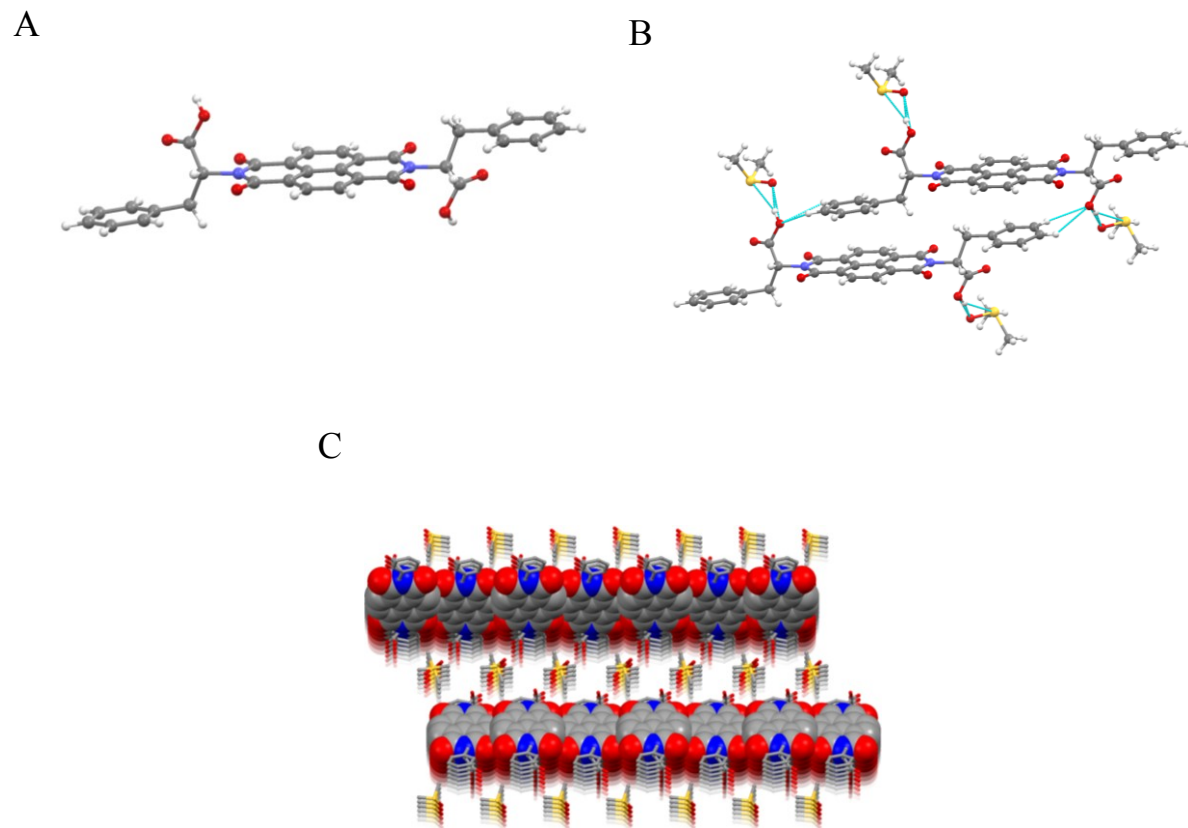


Fig. S9 A) Single molecular geometry of D-FNF indicating the *trans* conformation of α -phenyl substituents (phenyl) with respect to NDI plan. B) van der Waals' contacts between the two successive brick-work π -stacks (cyan doted lines). C) D-FNF layers (NDI core spacefill representation) separated by solvent (DMSO) layers; viewed along *a* axis. hydrogen atoms have been omitted for the clarity.

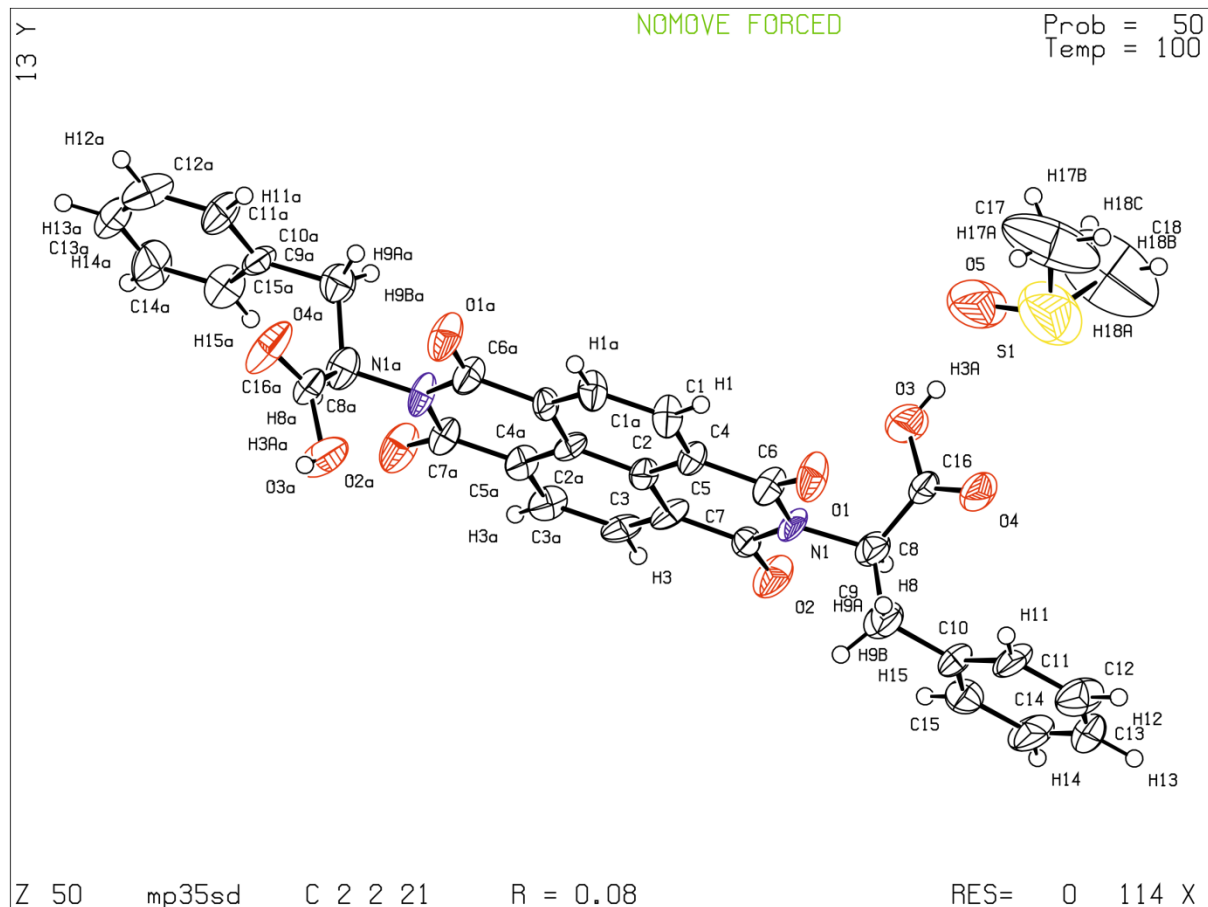


Fig. S10 ORTEP diagram of D-FNF

List of selected noncovalent interactions in D-FNF crystal structure

$\pi \cdots \pi$ stacking

Ring1	Ring 2	Distance (Å)	Angle between two NDI planes (°)	Description
Phenyl ring (Centroid)	NDI core unit	3.46	5.30	Intermolecular $\pi \cdots \pi$ interactions

Face to Face

Hydrogen bonds

Donor (D)	Acceptor (A)	D···A Distance (Å)	H···A Distance (Å)	D-H···A Angle (°)	Description
C12H12	O3	3.30	2.70	121.30	Aromatic (Phenyl) C -H···O (carboxylic acid) interactions
C13H13	O3	3.30	2.71	121.17	
C3H3	O1	3.34	3.07	98.03	Intermolecular Aromatic (NDI) C-H···O (carbonyl of NDI) interactions
C1H1	O2	3.34	3.02	101.36	

Interactions with solvent (DMSO) molecule

Hydrogen bonds

Donor (D)	Acceptor (A)	D···A Distance (Å)	H···A Distance (Å)	D-H···A Angle (°)	Description
O3H3A	O5	2.58	1.76	164.93	Intermolecular solvent (DMSO) O···molecule (carboxylic acid) interactions

van der Waals' contacts

van der Waals' contact	Distance (Å)	Description
H33A···H15	2.590	Intermolecular solvent (DMSO) C-H···H-C (α -CH of phenylalanine) interaction

CH··· π interactions

CH Donor (D)	Pi Acceptor (A)	D···A-centroid Distance (Å)	H···A-centroid Distance (Å)	D-H···A-centroid Angle (°)	Description
C17H17A	Phenyl ring	4.121	3.168	164.76	Intermolecular solvent (DMSO) C-H···Phenyl ring (phenylalanine) interaction

Molecular packing

- Intralayer along b axis: Brickwork
- Interlayer along c axis: Slipped herringbone

Angle between the layers: 66.10° (clockwise)

Crystallographic information of L-WNW

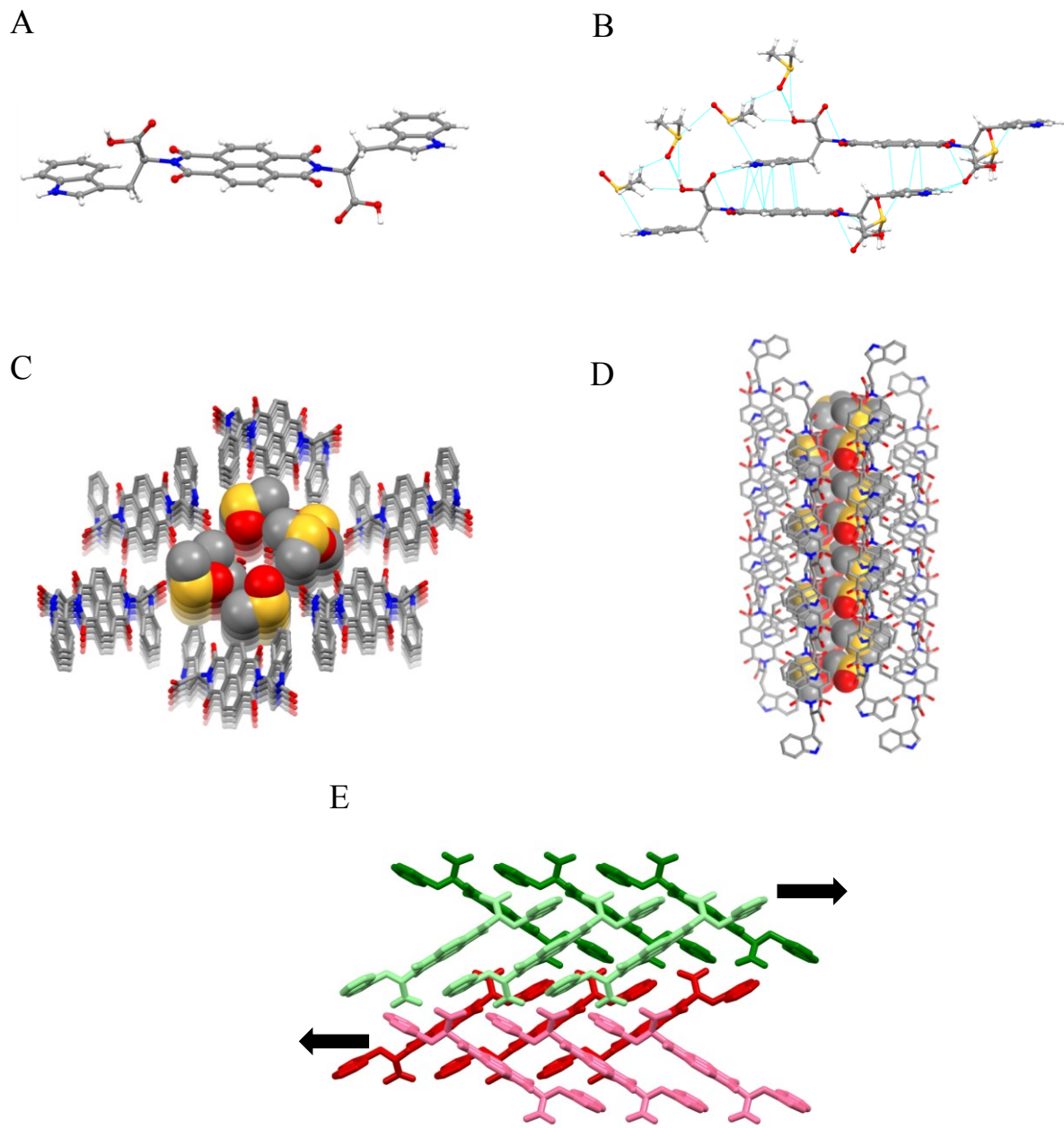


Fig. S11 A) Single molecular geometry of L-WNW indicating the *trans* conformation of c_{α} substituents (indole) with respect to NDI plan. B) van der Waals' contacts between the two successive molecules (cyan doted lines). C) and D) Solvent (DMSO, spacefill representation) channels in L-WNW; viewed along *a* axis and *b* axis respectively. E) Antiprallal adjacent 2_1 helices in L-WNW (solvent not shown in crystal packing for the clarity). In C-E hydrogen atoms have been omitted for the clarity.

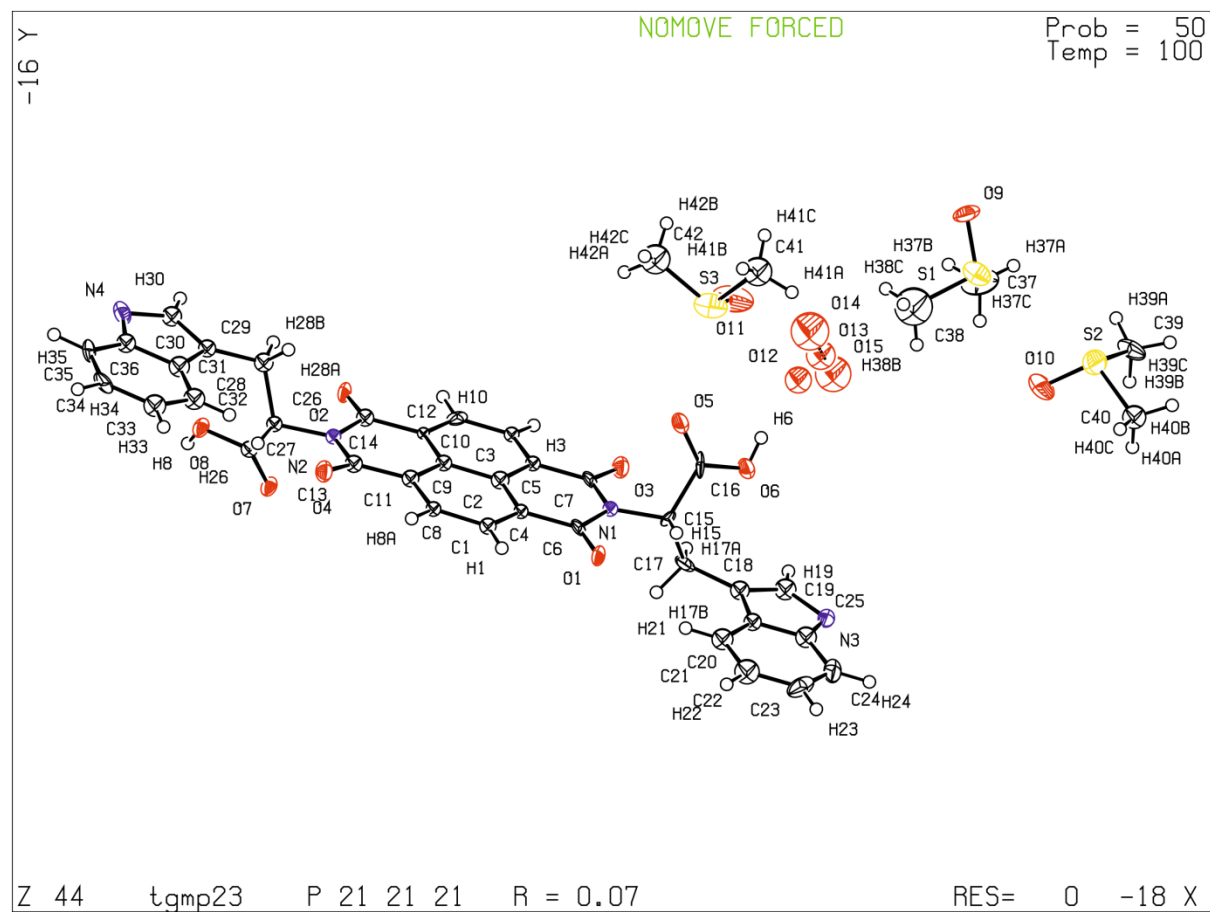


Fig. S12 ORTEP diagram of L-WNW

List of selected noncovalent interactions in L-WNW crystal structure

Ring1	Ring 2	Distance (Å)	Angle between two NDI planes (°)	Description
Tryptophan ring (centroid)	NDI core unit	3.20	6.03	Intermolecular aromatic Donor (Trp)…Acceptor (NDI) Charge transfer $\pi\cdots\pi$ interactions

Hydrogen bonds

Donor (D)	Acceptor (A)	D…A Distance (Å)	H…A Distance (Å)	D-H…A Angle (°)	Description
N3H43	O5	2.89	2.04	161.73	Intermolecular N-H (indole ring)…O (carboxylic acid) hydrogen bonding interactions
N4H44	O7	2.88	2.05	157.03	
C30H30	O2	3.53	2.60	163.61	Intermolecular Aromatic (indole) C-H…O (carbonyl of NDI) interactions
C3H3	O7	3.53	2.63	158.35	Intermolecular Aromatic (NDI) C-H…O (carboxylic acid) interactions
C10H10	O8	3.35	2.70	125.44	

C33H33	O5	3.31	2.59	132.04	Intermolecular Aromatic (indole) C-H···O (carboxylic acid) interactions
C24H24	Indole ring	4.58	3.65	166.86	Intermolecular C-H (indole) ... π (indole) interactions

Interactions with solvent (DMSO) molecule

Hydrogen bonds

Donor (D)	Acceptor (A)	D···A Distance (Å)	H···A Distance (Å)	D-H···A Angle (°)	Description
O8H8	O9	2.52	1.70	164.52	Intermolecular solvent (DMSO) O···molecule (carboxylic acid) interactions

Molecular packing

- Interlayer along *c* axis: herringbone

Angle between the layers: 64.36° (anti-clockwise)

Geometric parameters for supramolecular tilt helices

parameter	eNe	L-FNF	D-FNF	L-WNW
Helix direction	<i>c</i>	<i>c</i>	<i>c</i>	<i>a</i>
Helix pitch (Å)	18.38	27.66	28.20	8.67
Centroid - Helix axis distance (Å)	3.11	3.14	3.32	3.33
Tilt angle (°)	44.63	66.09	66.15	115.64

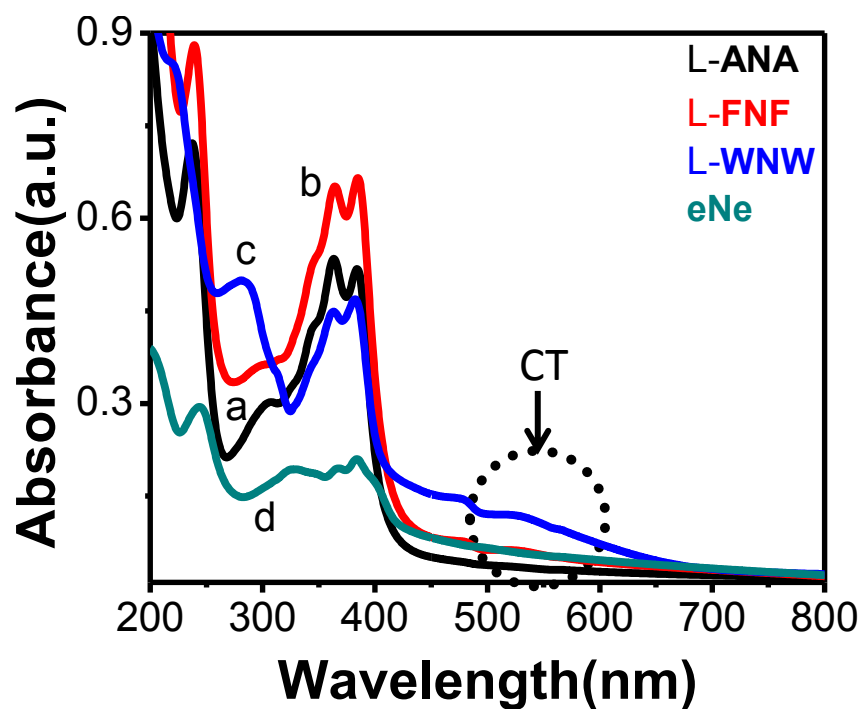


Fig. S13 UV-vis absorption spectra of NDI-conjugates recorded on their respective thin films.

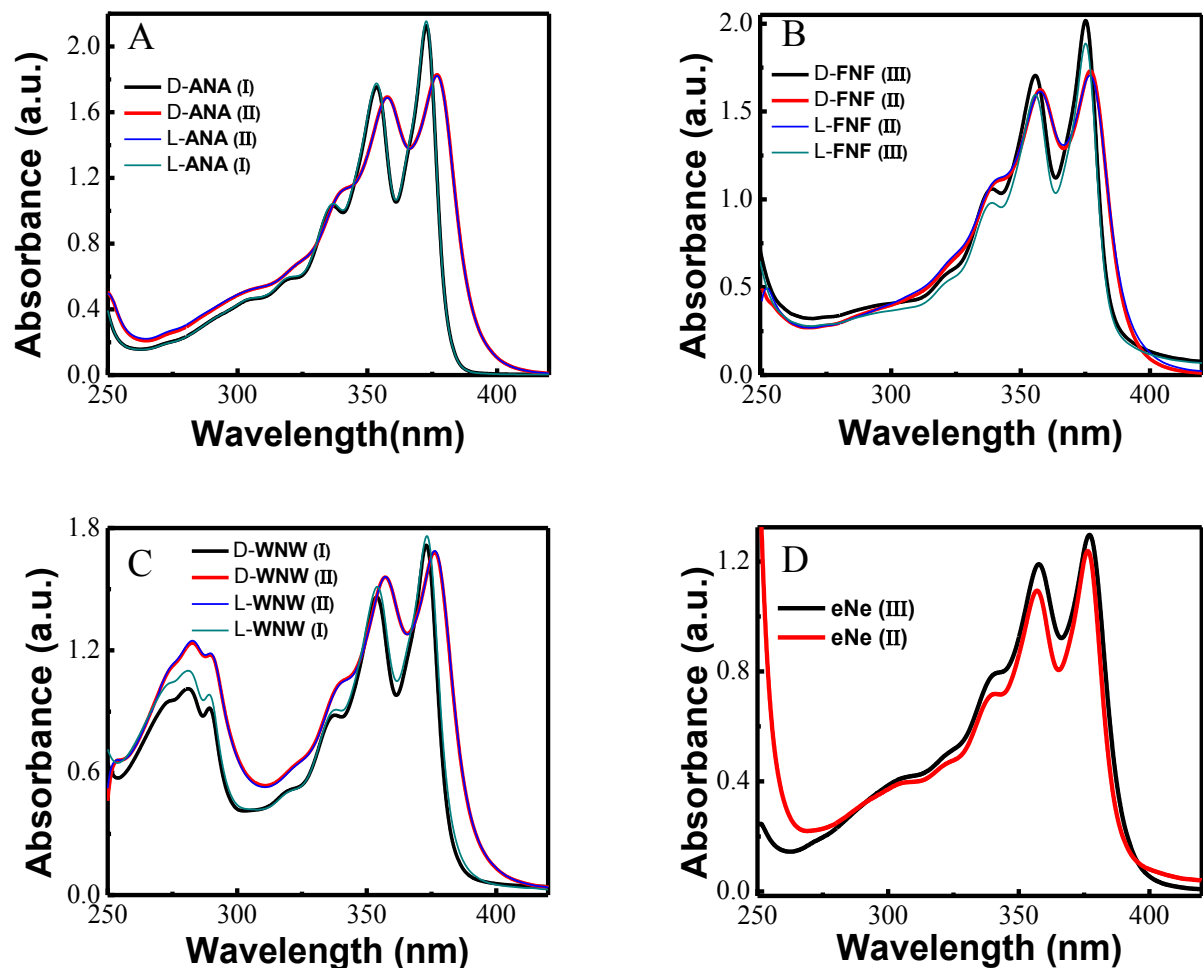


Fig. S14 UV-vis absorption spectra of NDI-conjugates. A) L-ANA and D-ANA. B) L-FNF and D-FNF. C) L-WNW and D-WNW. D) eNe. (I: MCH/THF II: DMSO and III: MCH/CHCl₃).

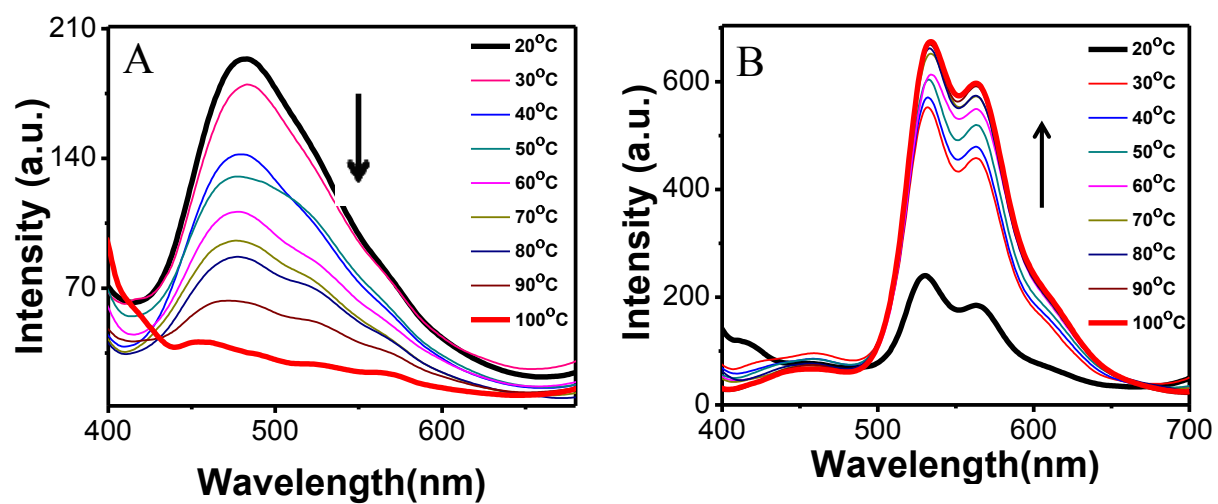


Fig. S15 Temperature dependent fluorescence emission spectra of L-FNF and eNe.

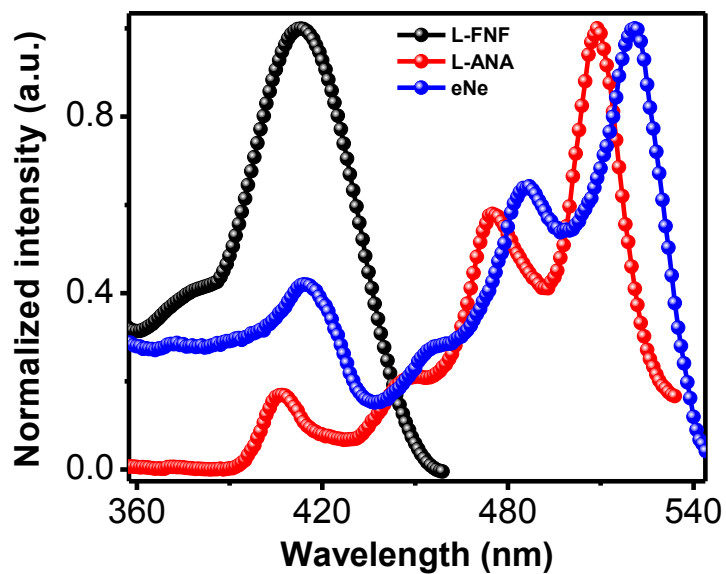


Fig. S16 Excitation spectra of L-FNF (at $\lambda_{\text{emission}} = 490$ nm), L-ANA (at $\lambda_{\text{emission}} = 552$ nm) and eNe (at $\lambda_{\text{emission}} = 563$ nm) in their solid state.

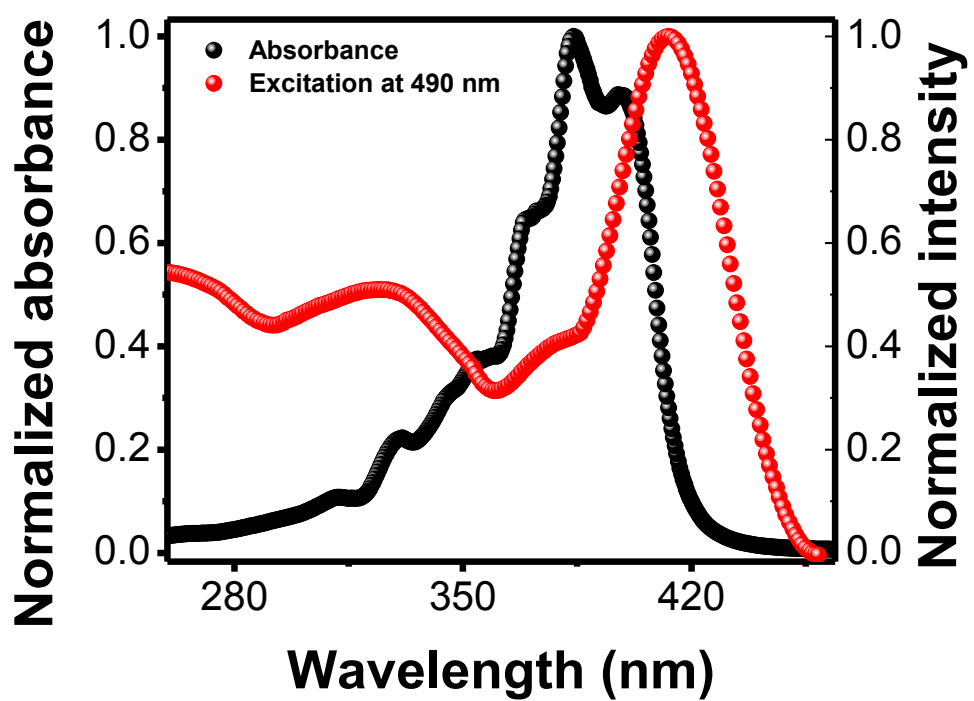


Fig. S17 UV-vis absorption (260- 460 nm region) and excitation spectra (at $\lambda_{\text{emission}} = 490 \text{ nm}$) of L-FNF in solid state.

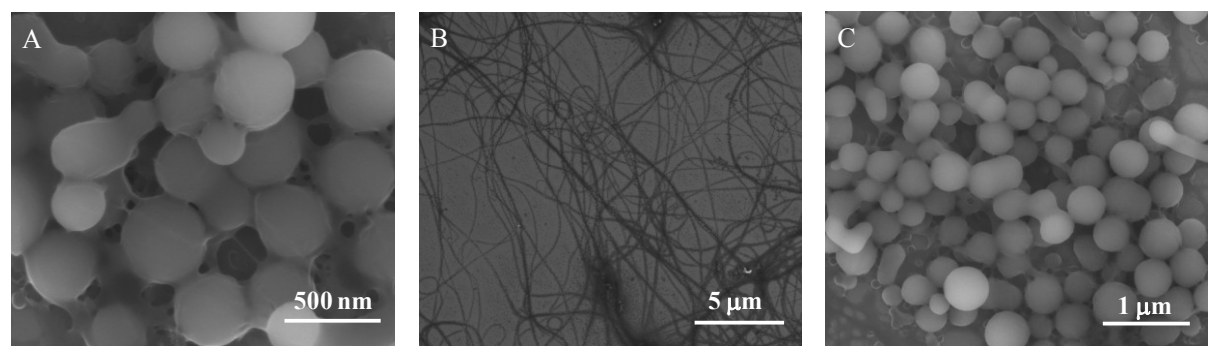
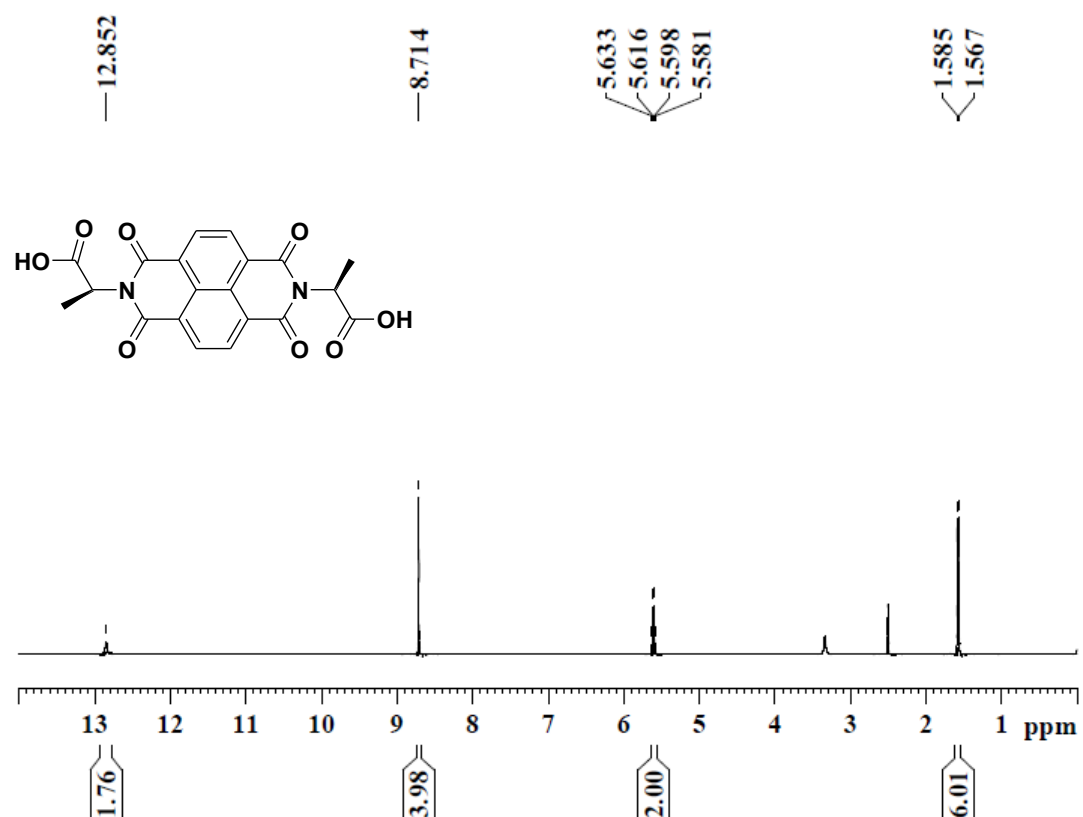
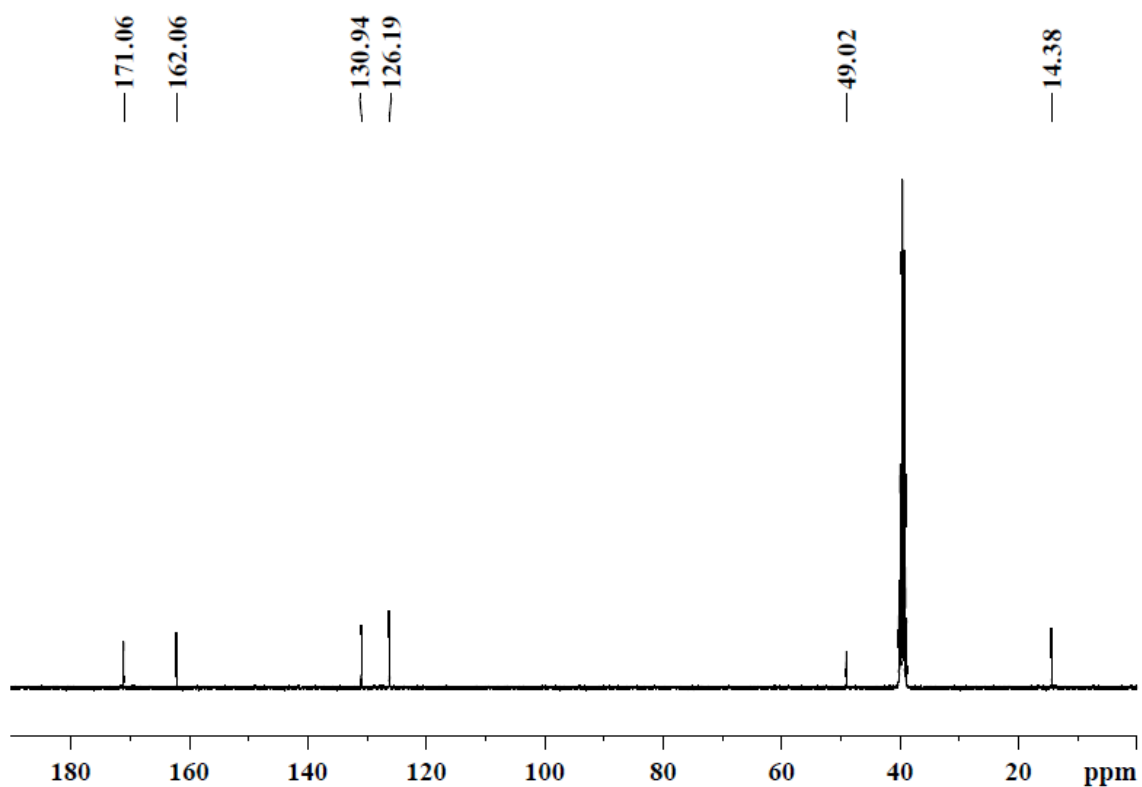


Fig. S18 FESEM micrographs of solutions of **ANA** (A), **FNF** (B), and **WNW** (C).

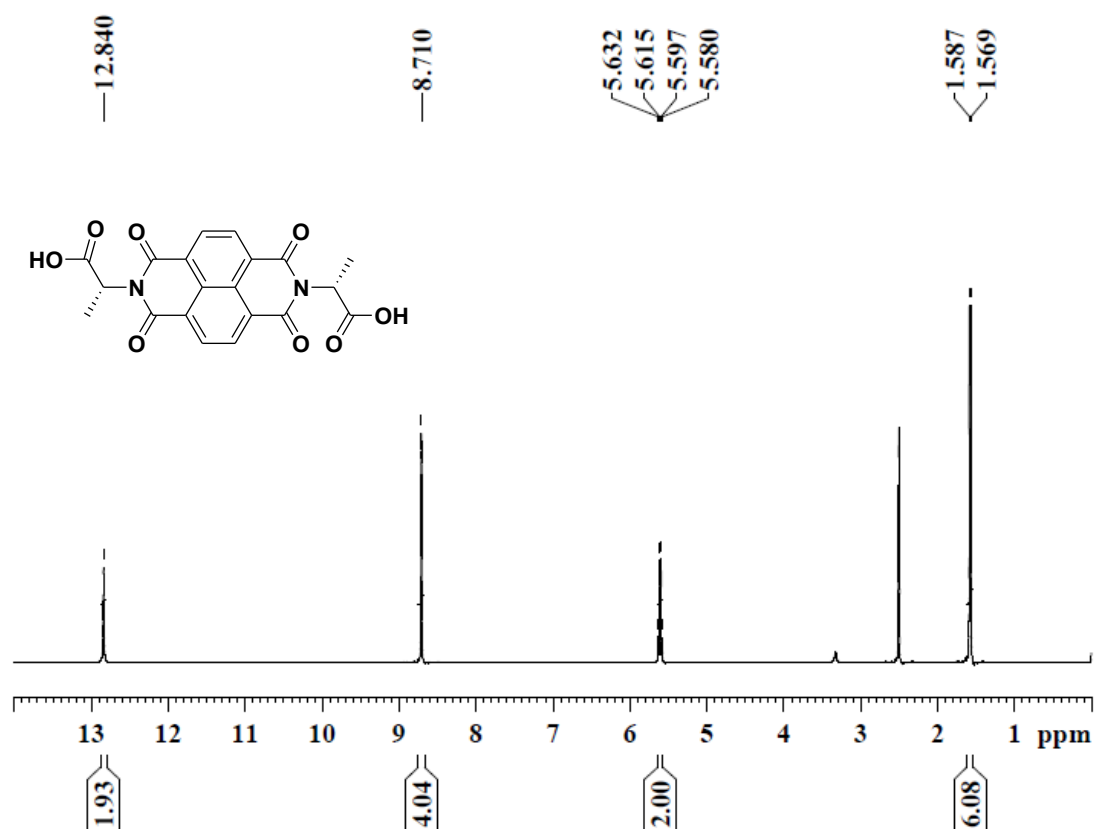
¹H NMR spectrum (*DMSO-d*₆, 400 MHz) of L-ANA



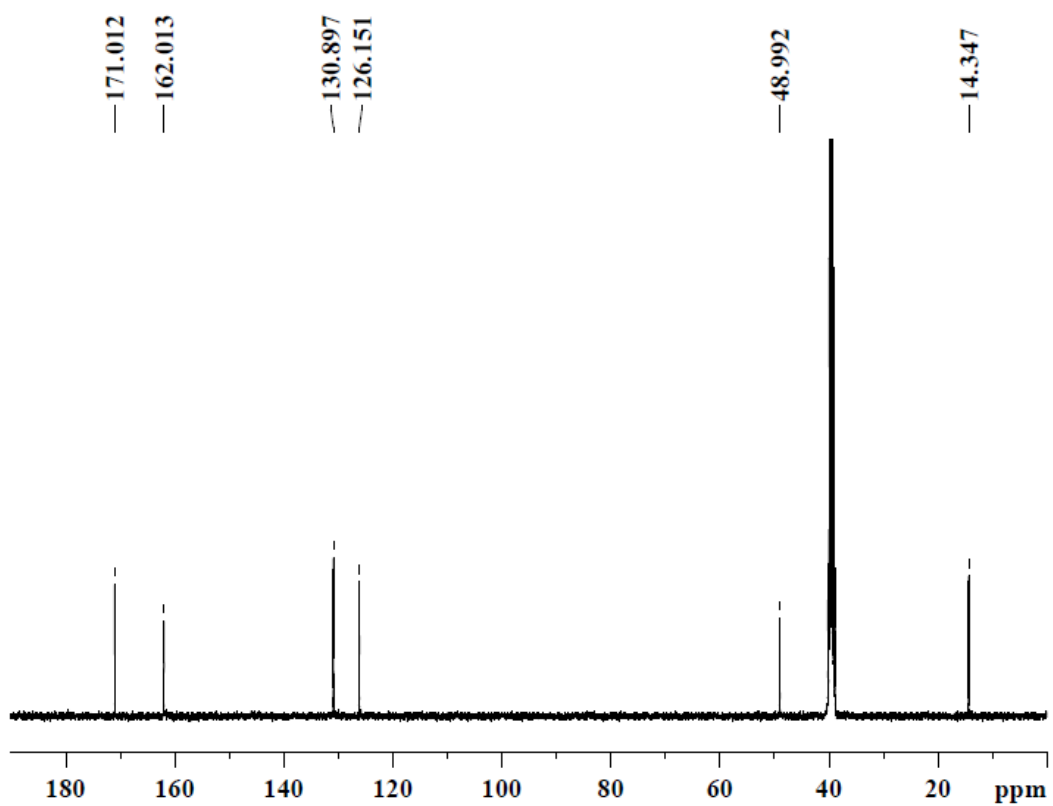
¹³C NMR spectrum (*DMSO-d*₆, 100 MHz) of L-ANA



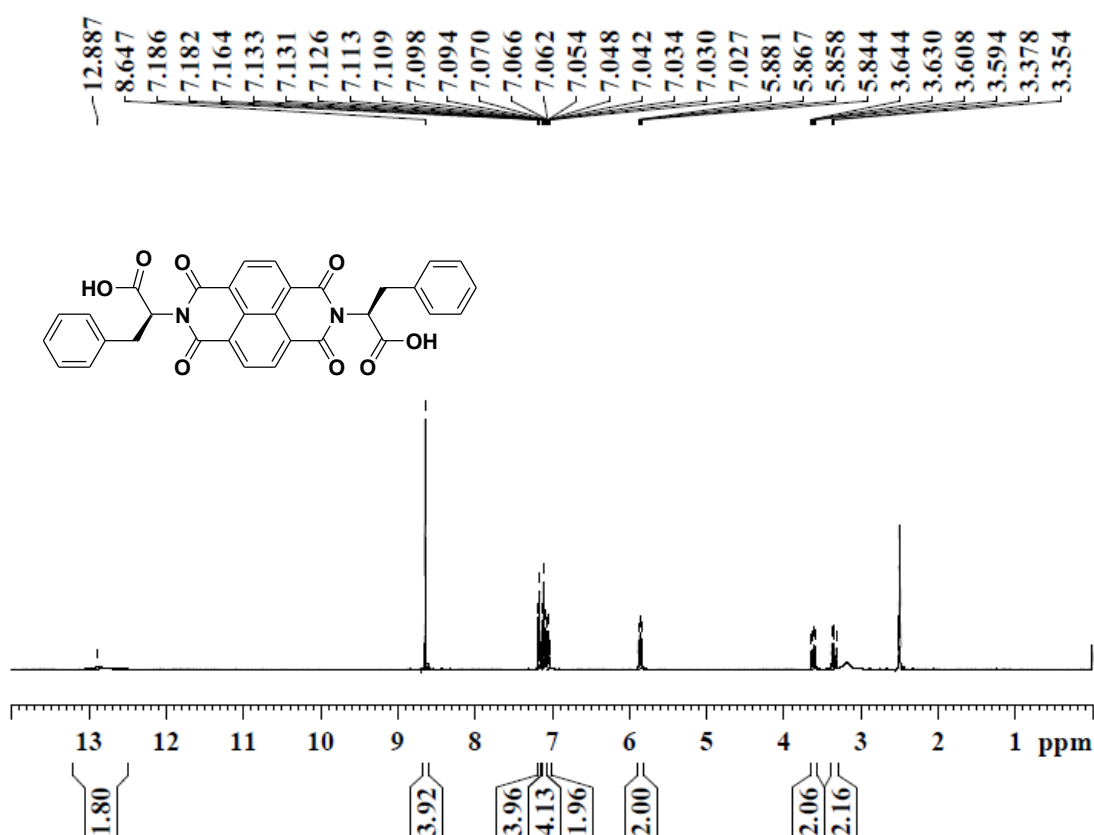
¹H NMR spectrum (*DMSO-d*₆, 400 MHz) of D-ANA



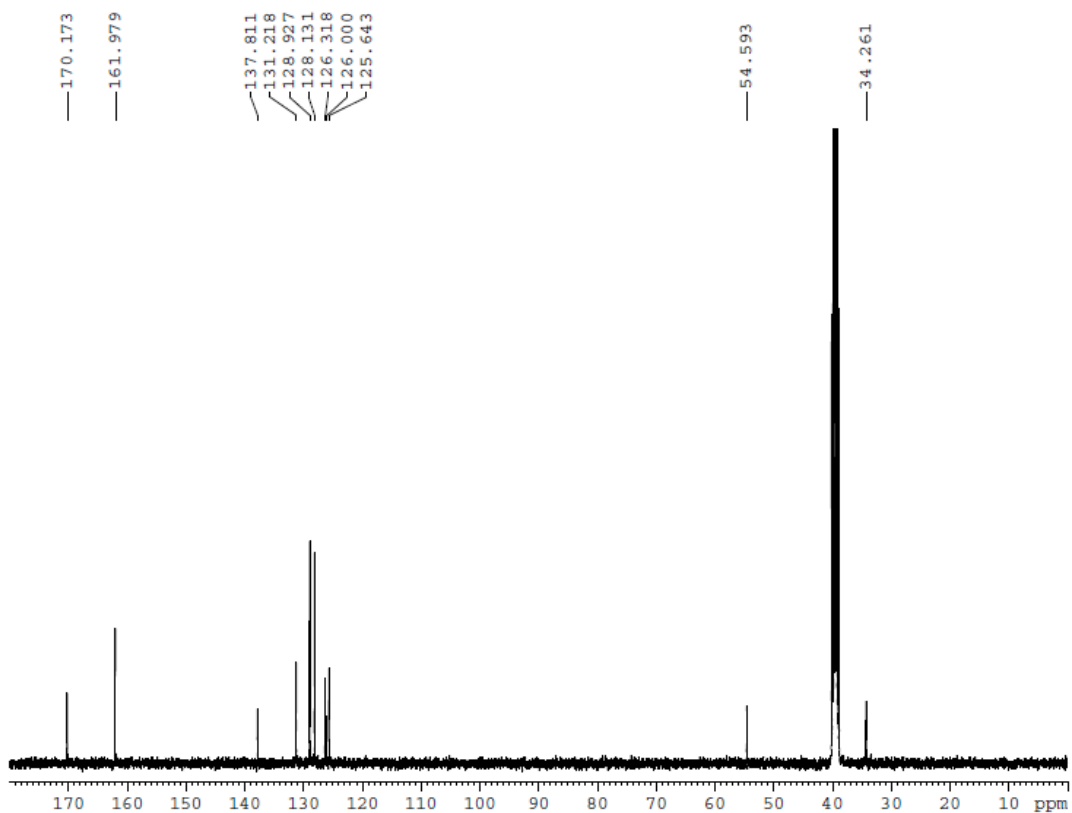
¹³C NMR spectrum (*DMSO-d*₆, 100 MHz) of D-ANA



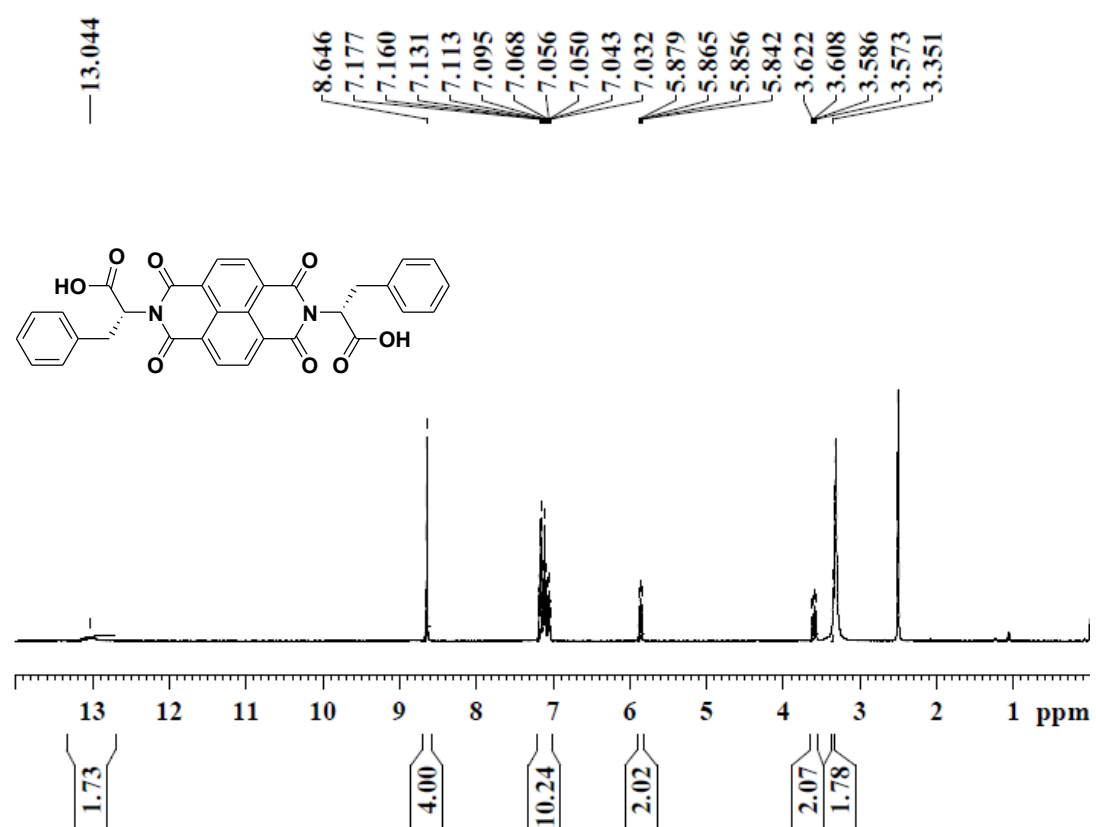
¹H NMR spectrum (*DMSO-d*₆, 400 MHz) of L-FNF



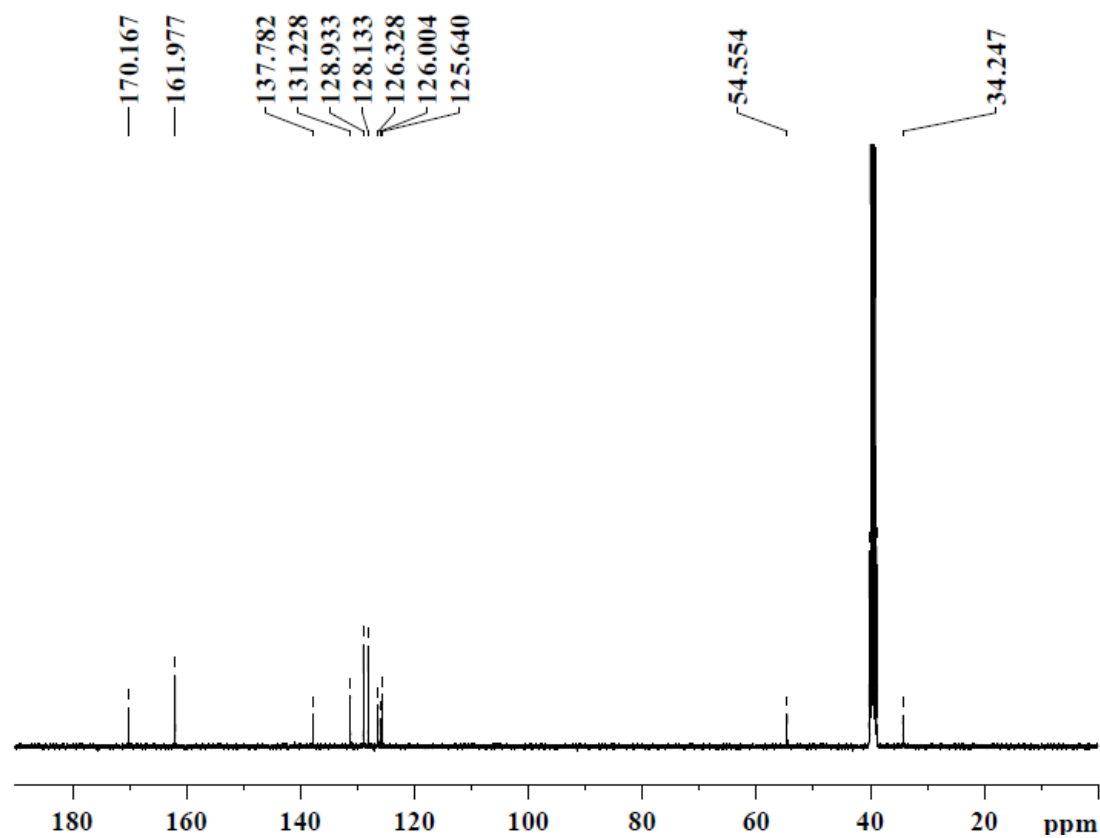
¹³C NMR spectrum (*DMSO-d*₆, 100 MHz) of L-FNF



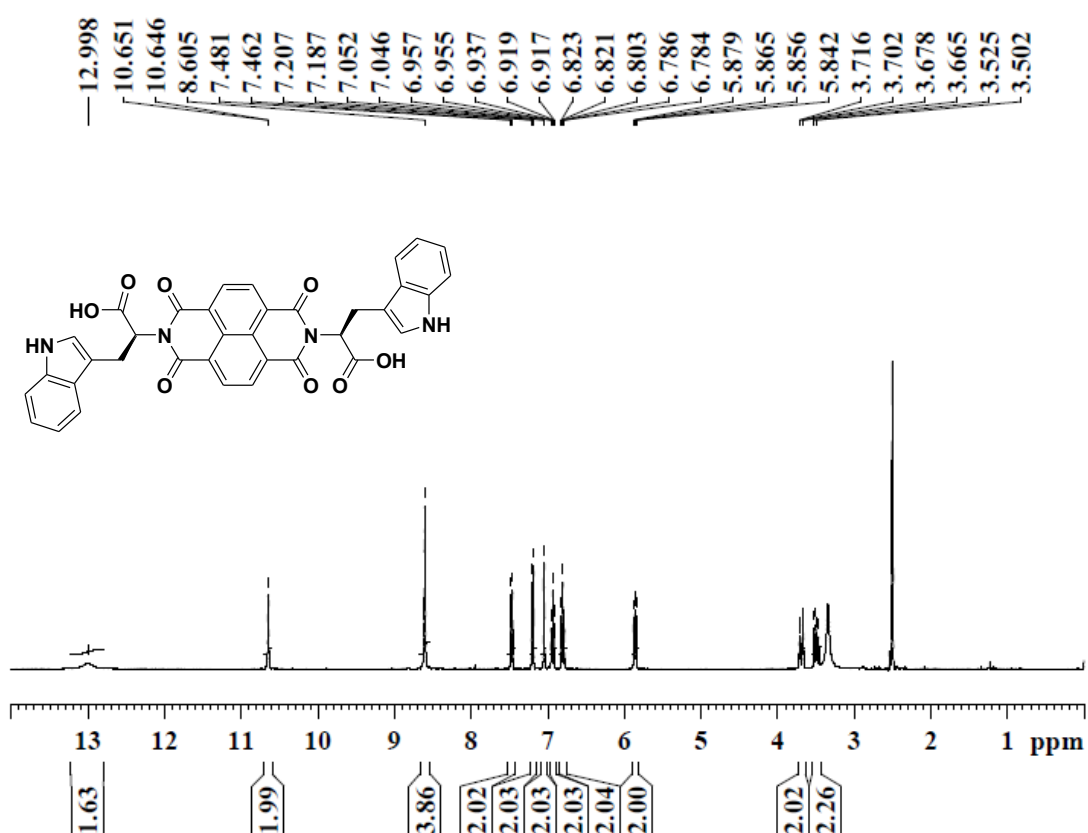
¹H NMR spectrum (*DMSO-d*₆, 400 MHz) of D-FNF



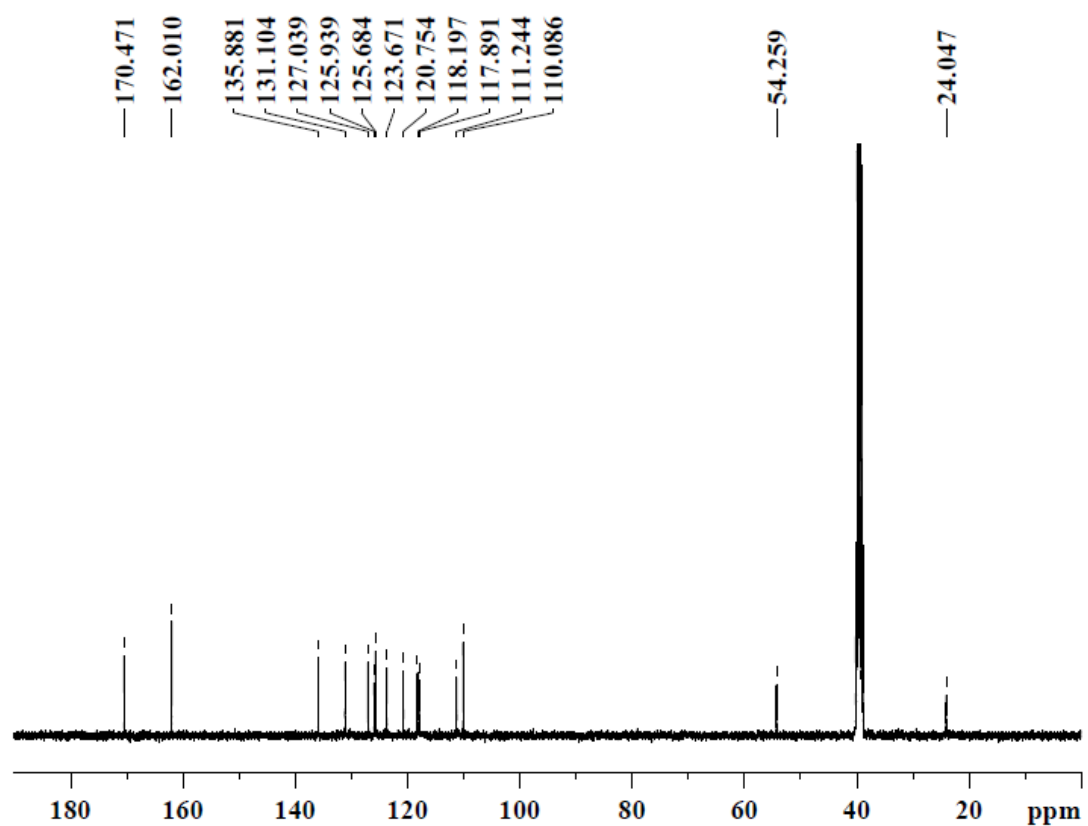
¹³C NMR spectrum (*DMSO-d*₆, 100 MHz) of D-FNF



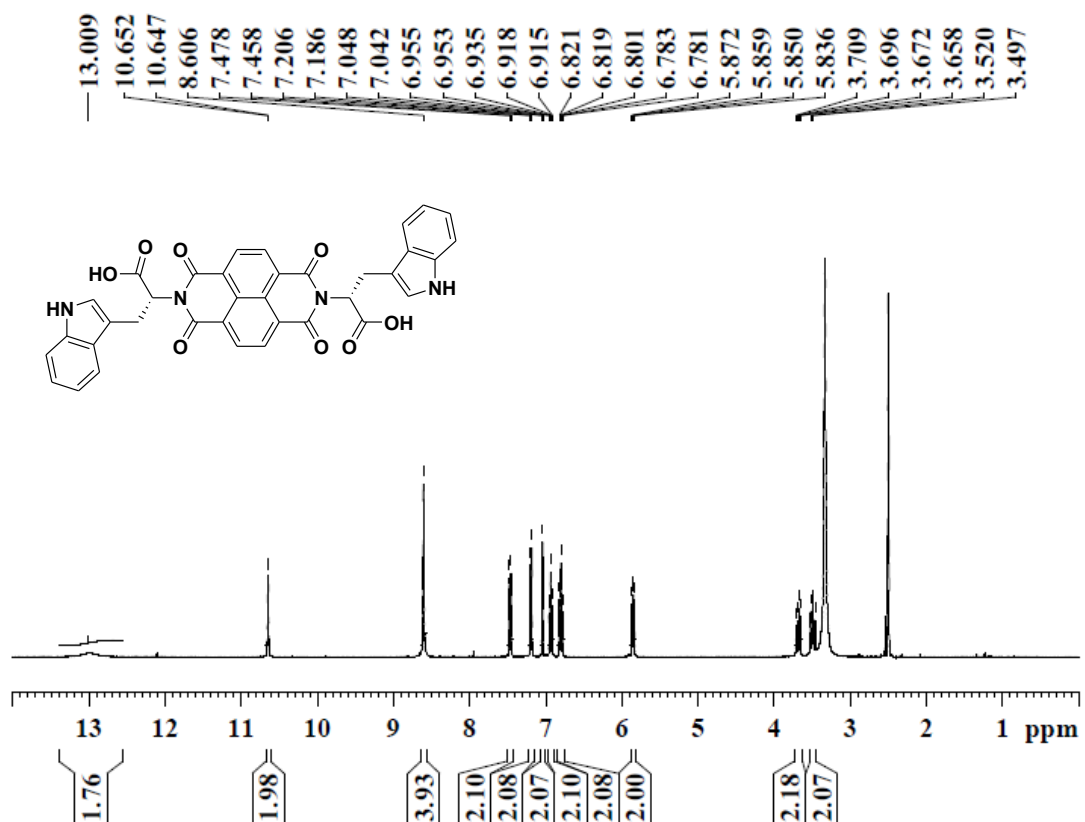
¹H NMR spectrum (*DMSO-d*₆, 400 MHz) of L-WNW



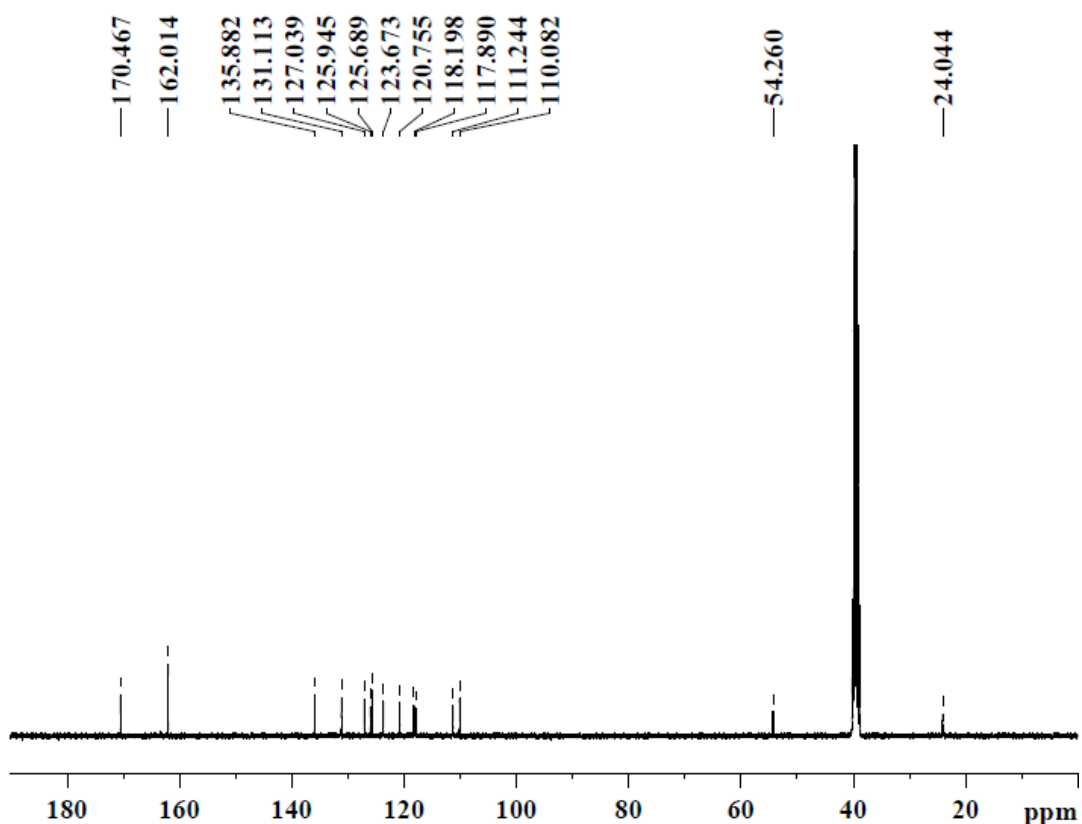
¹³C NMR spectrum (*DMSO-d*₆, 100 MHz) of L-WNW



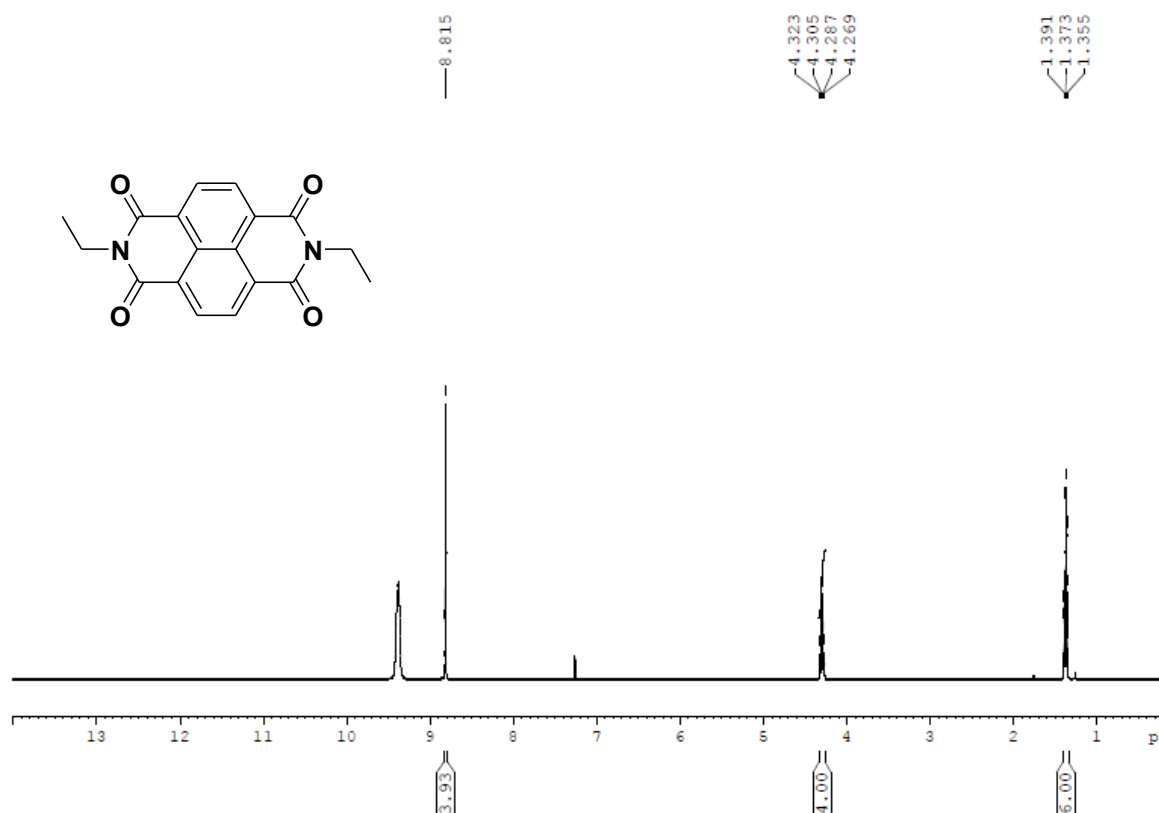
¹H NMR spectrum (*DMSO-d*₆, 400 MHz) of D-WNW



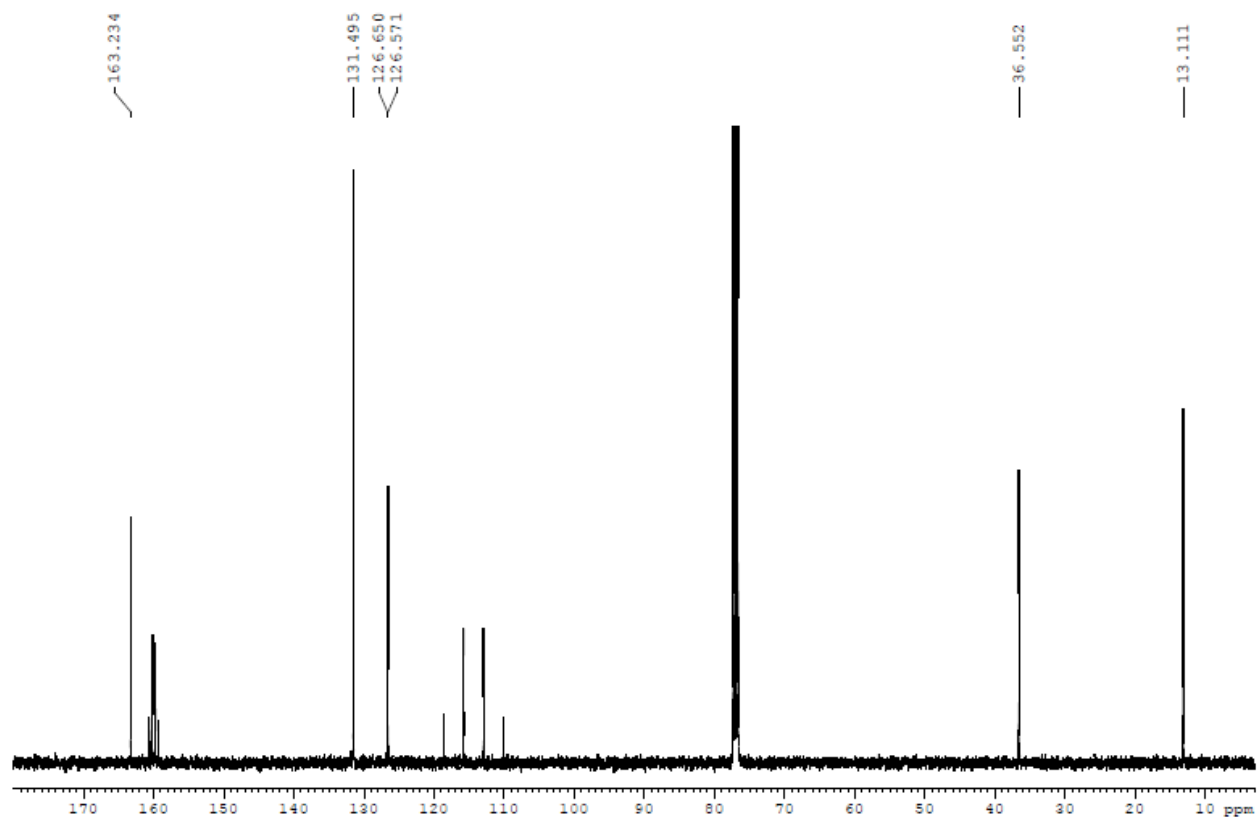
¹³C NMR spectrum (*DMSO-d*₆, 100 MHz) of D-WNW



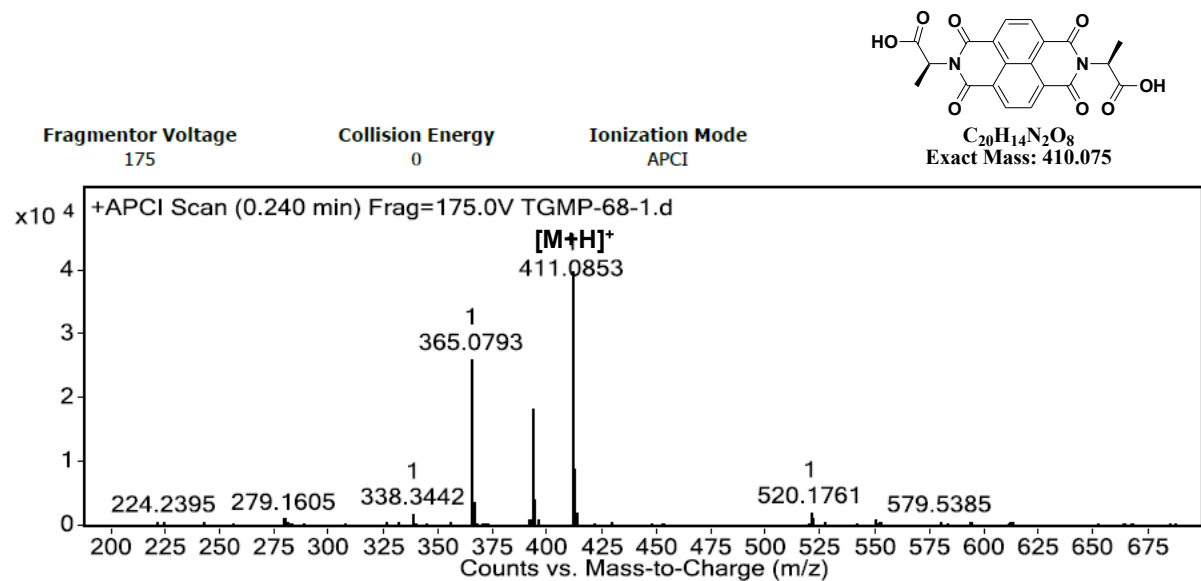
¹H NMR spectrum (*CDCl*₃+TFA(3μL), 400 MHz) of eNe



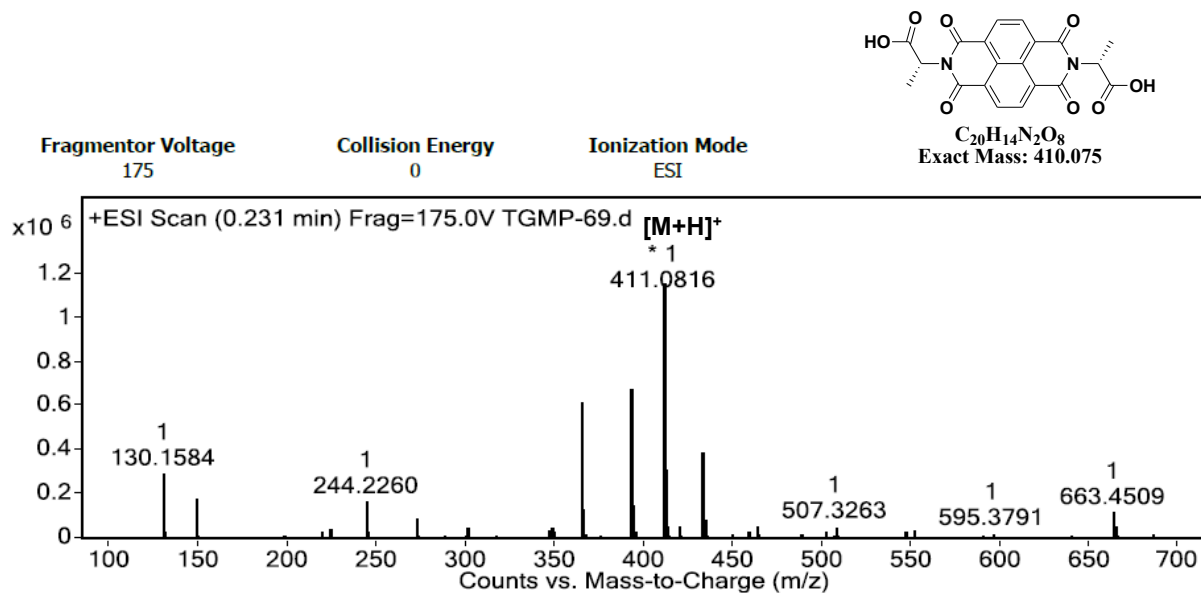
¹³C NMR spectrum (*CDCl*₃+TFA (3μL), 100 MHz) of eNe



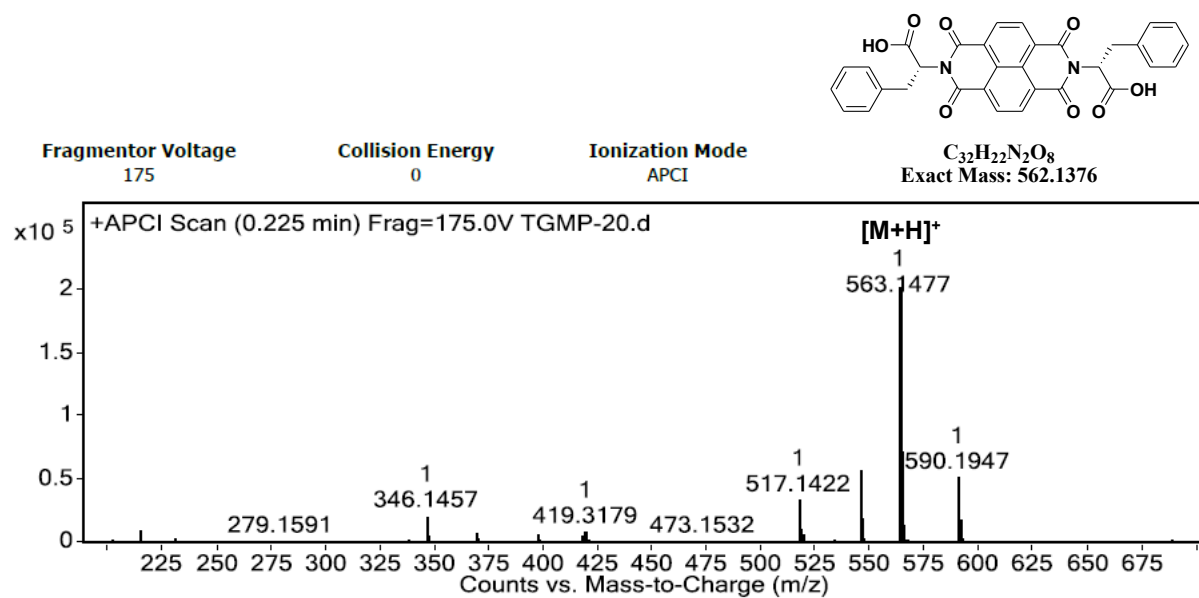
HRMS spectrum of L-ANA



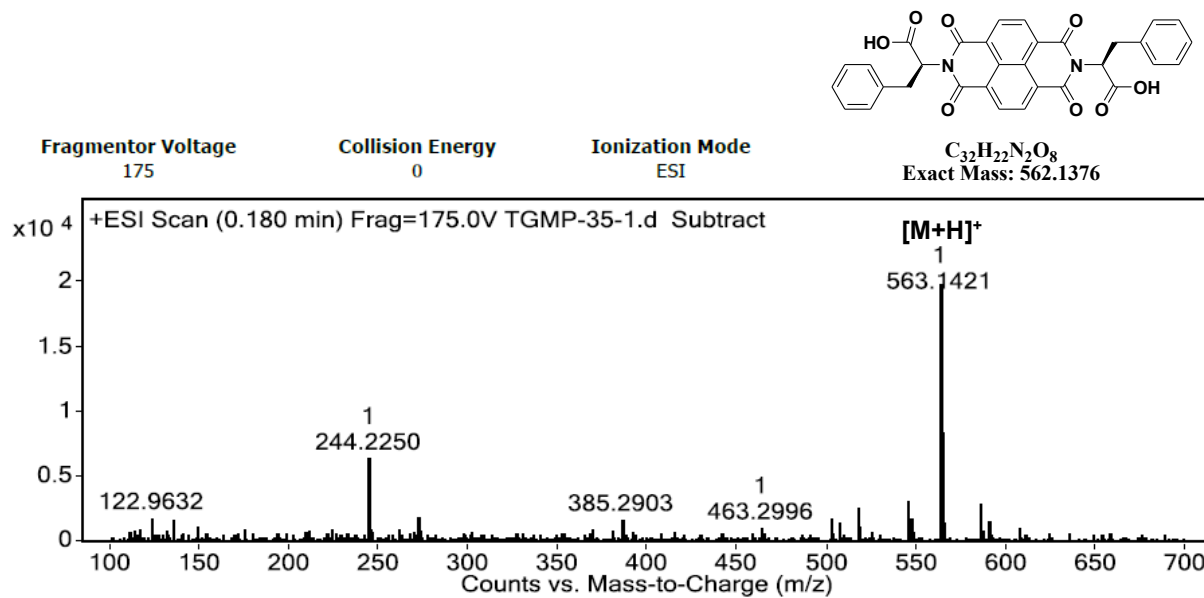
HRMS spectrum of D-ANA



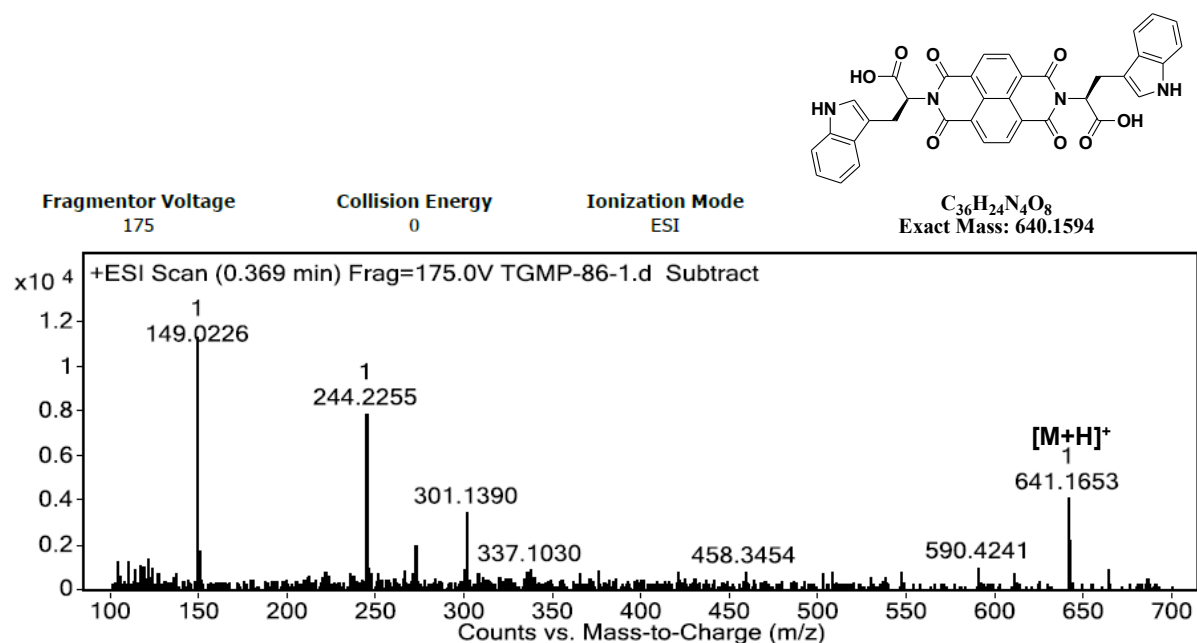
HRMS spectrum of L-FNF



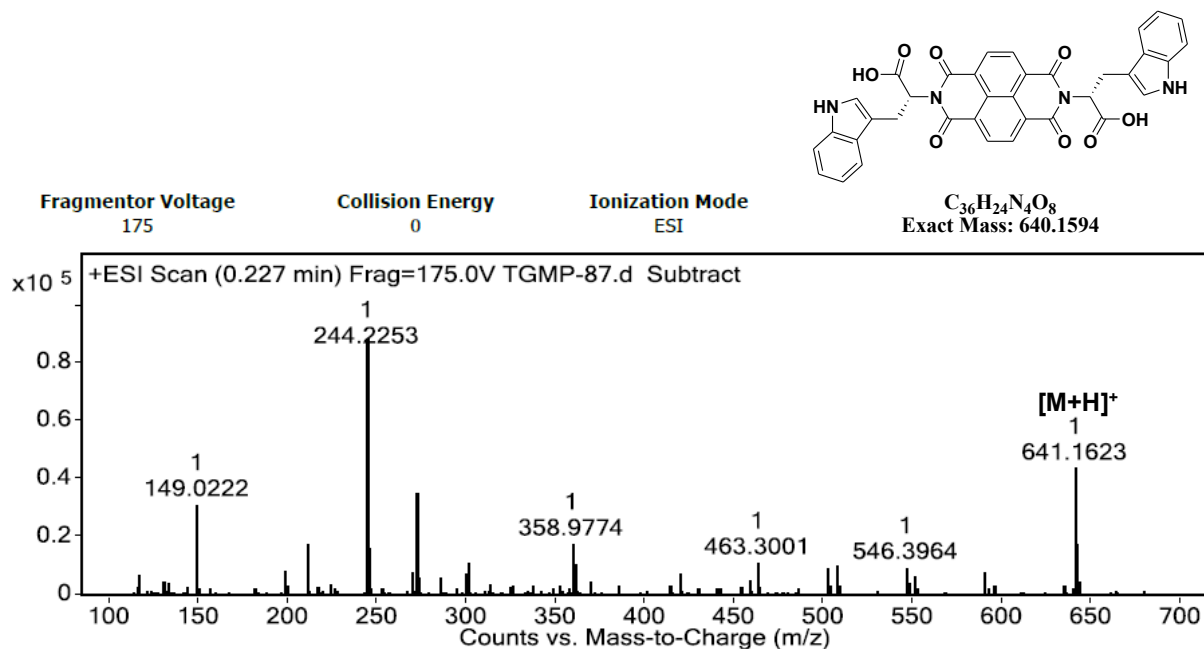
HRMS spectrum of D-FNF



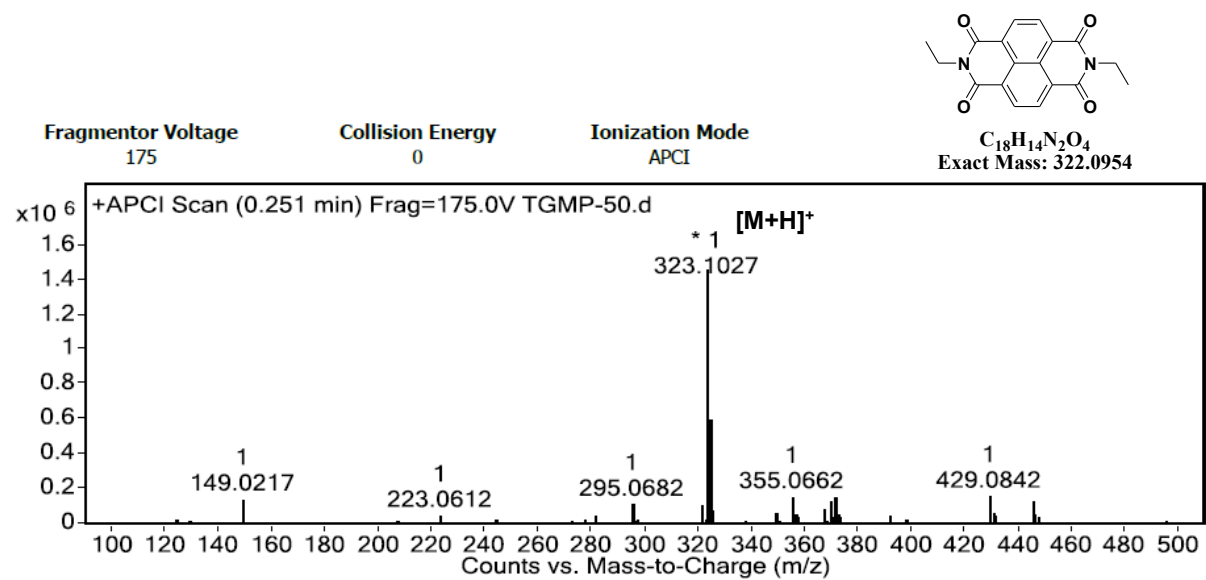
HRMS spectrum of L-WNW



HRMS spectrum of D-WNW



HRMS spectrum of eNe



References:

- (1) SHELXS-2013, A program for automatic solution of crystal structures, University of Göttingen, Göttingen.
- (2) SHELXL-2013, A program for crystal structure refinement, University of Göttingen, Göttingen.
- (3) WinGX package; L. J. Farrugia, *J. Appl. Cryst.* 2012, **45**, 849-854.